University of New Mexico
UNM Digital Repository

Mechanical Engineering ETDs Engineering ETDs

9-3-2013

Effects of underfill material on solder deformation and damage in 3D packages

Geno Flores

Follow this and additional works at: https://digitalrepository.unm.edu/me_etds

Recommended Citation
Flores, Geno. "Effects of underfill material on solder deformation and damage in 3D packages." (2013).
https://digitalrepository.unm.edu/me_etds/73

This Thesis is brought to you for free and open access by the Engineering ETDs at UNM Digital Repository. It has been accepted for inclusion in Mechanical Engineering ETDs by an authorized administrator of UNM Digital Repository. For more information, please contact disc@unm.edu.

Geno C. Flores

Candidate

Mechanical Engineering

Department

This thesis is approved, and it is acceptable in quality and form for publication:

Approved by the Thesis Committee:

Yu-Lin Shen , Chairperson

Tariq Khraishi

Arsalan Razani

Effects of Underfill Material on Solder Deformation and Damage in 3D Packages

by

Geno C. Flores

B.S., Mechanical Engineering, University of New Mexico, 2010

THESIS

Submitted in Partial Fulfillment of the
Requirements for the Degree of

Master of Science
Mechanical Engineering

The University of New Mexico

Albuquerque, New Mexico

June, 2013

©2013, Geno C. Flores

Dedication

For my wife, my family, and my friends who have always believed in me.

Acknowledgments

I wish to thank my advisor, Dr. Yu-Lin Shen, as well as Dr. Tariq Khraishi and Dr. Arsalan Razani for serving on my committee.

In addition, I would like to thank Professor Robert Greenlee, whose willingness to look beyond a poor transcript is the reason that I am able to have this opportunity to defend this research, as well as everyone who has supported me in this endeavor.

Effects of Underfill Material on Solder Deformation and Damage in 3D Packages

by

Geno C. Flores

B.S., Mechanical Engineering, University of New Mexico, 2010

M.S., Mechanical Engineering, University of New Mexico, 2013

Abstract

This paper will examine the effects of the introduction of a periodic boundary condition and the presence of underfill material on the stress and strain fields and evolution of failure of an FEA model that is representative of a solder joint in a 3D IC package. The model solder joint is placed between two silicon substrates in contact with through-silicon vias without any other devices or components attached. Differing solder joint thicknesses, both with and without underfill, will be examined to study the effect on the stress and strain fields as well as the evolution of failure in the solder joint. A dynamic loading on the FEA model will be used to examine the fracture pattern and mode of failure when the solder thickness is varied both with and without underfill material present.

Contents

List of Figures **viii**

List of Tables **xiii**

1 Introduction **1**

2 Numerical Model **7**

3 Results: Periodic vs. Non-Periodic Boundary Condition **14**

4 Results: Solder Joint Fracture and Mode of Failure **31**

5 Concluding Discussion **46**

List of Figures

2.1 *Drawing of a 3D IC chip stack and a single interior solder joint. Symmetry is used to simplify the model.* 8

3.1 *Abaqus model showing von Mises stress without underfill present for a 5 micron solder joint with periodic B/C on the left and non-periodic B/C on the right. A plot of load versus displacement is included for comparison.* 15

3.2 *Abaqus models showing shear stress and equivalent plastic strain without underfill present for a 5 micron solder joint. The models with the periodic boundary condition are on the left and the non-periodic boundary condition models are on the right.* 16

3.3 *Abaqus model showing von Mises stress without underfill present for a 10 micron solder joint with periodic B/C on the left and non-periodic B/C on the right. A plot of load versus displacement is included for comparison.* 17

3.4 *Abaqus models showing shear stress and equivalent plastic strain without underfill present for a 10 micron solder joint. The models with the periodic boundary condition are on the left and the non-periodic boundary condition models are on the right.* 18

3.5 *Abaqus model showing Mises stress without underfill for a 20 micron solder joint with periodic B/C on the left and non-periodic B/C on the right. A plot of load versus displacement is included for comparison.* 19

3.6 *Abaqus models showing shear stress and equivalent plastic strain without underfill present for a 20 micron solder joint. The models with the periodic boundary condition are on the left and the non-periodic boundary condition models are on the right.* 20

3.7 *Abaqus model showing Mises stress with underfill present for a 5 micron solder joint with periodic B/C on the left and non-periodic B/C on the right. A plot of load versus displacement is included for comparison.* 21

3.8 *Abaqus models showing shear stress and equivalent plastic strain with underfill present for a 5 micron solder joint. The models with the periodic boundary condition are on the left and the non-periodic boundary condition models are on the right.* 22

3.9 *Abaqus model showing von Mises stress with underfill present for 10 micron solder joint with periodic B/C above and non-periodic B/C below. A plot of load versus displacement is included for comparison.* 23

3.10 *Abaqus models showing shear stress and equivalent plastic strain with underfill present for a 10 micron solder joint. The models with the periodic boundary condition are on the left and the non-periodic boundary condition models are on the right.* 24

3.11 *Abaqus model showing von Mises stress with underfill present for 20 micron solder joint with periodic B/C on the left and non-periodic B/C on the right. A plot of load versus displacement is included for comparison.* 25

3.12 *Abaqus models showing shear stress and equivalent plastic strain with underfill present for a 20 micron solder joint. The models with the periodic boundary condition are on the left and the non-periodic boundary condition models are on the right.* 26

3.13 *Plots of load versus displacement for the test cases without underfill present for the test cases that included a periodic boundary condition. Note that although the 5 micron solder joint is able to resist a higher loading than the 10 or 20 micron joints.* 29

3.14 *Plots of load versus displacement for the test cases with underfill present for the test cases that included a periodic boundary condition. Note that the 5 micron solder joint is able to resist a higher loading than the 10 or 20 micron joints.* 30

4.1 *Abaqus model showing the failure of the 5 micron solder joint without underfill present. The load versus displacement curve showing the significant drop in loading at approximately 1.5 microns indicates that the joint has failed.* 32

4.2 *Abaqus model showing the failure of the 10 micron solder joint without underfill present. The load versus displacement curve showing the significant drop in loading at approximately 2.5 microns indicates that the joint has failed.* 33

4.3 *Abaqus model showing the failure of the 20 micron solder joint without underfill present. The load versus displacement curve showing the significant drop in loading at approximately 3.5 microns indicates that the joint has failed.* 36

4.4 *Abaqus model showing the failure of the 5 micron solder joint with underfill present. The load versus displacement curve does not show any significant drop in loading due to the fact that the underfill material continues to resist the loading even after the joint has failed.* . . 37

4.5 *Abaqus model showing the failure of the 10 micron solder joint with underfill present. The load versus displacement curve does not show any significant drop in loading due to the fact that the underfill material continues to resist the loading even after the joint has failed.* . . 39

4.6 *Abaqus model showing the failure of the 20 micron solder joint with underfill present. The load versus displacement curve does not show any significant drop in loading due to the fact that the underfill material continues to resist the loading even after the joint has failed.* . . 40

4.7 *Abaqus model of the 5 micron solder joint with underfill present. This model utilized a much finer mesh incorporating four times the number of elements used in the other test case models. The results of the simulation are much more in agreement with the other two test cases with underfill present. A plot of load versus displacement is included for comparison.* 41

4.8 *Plots of load versus displacement for the test cases without underfill present. Note that although the 5 micron solder joint has failed first, it actually resisted a higher loading before failure.* 42

4.9 *Plots of load versus displacement for the test cases with underfill present. Note that the 5 micron solder joint is able to resist a higher loading than the 10 or 20 micron solder joints.* 43

5.1 *Plots of load versus displacement for all of the test cases in the first part of this research. Note that the 5 micron solder joint with underfill present is able to resist a higher loading than any of the other test cases.* 48

5.2 *Plots of load versus displacement for all of the test cases in the second part of this research. Note that the 5 micron solder joint with underfill present is able to resist a higher loading than any of the other test cases.* 49

List of Tables

2.1 Material Properties 9

5.1 Failure Time And Displacement Without Underfill Present 46

5.2 Failure Time And Displacement With Underfill Present 47

Chapter 1

Introduction

As computer technology advances, the inevitable pinnacle of the state of the art becomes more and more unavoidable. Termed Moore's Law, the concept revolves around the fact that the power of the integrated circuit will eventually reach a point where engineers can no longer increase the computing power of the integrated circuits. It states that the density of 2-D integrated circuits on silicon chips will double every 18-25 months and has been valid for the last 30-40 years. For example, in the case of memory chips we can say that the number of devices on a chip was at 1K, or one thousand, in 1975 and reached one million per chip in 1990. This represents an increase of three orders of magnitude and took 15 years. As a check on the validity of Moore's law, we have 2^{10} = 1,024 and 2^{20} = 1,048,576 which represents a doubling occurring ten times. Moore's law states that it should take 10 x 18 months = 15 years, which is approximately how long it did take. The same holds true for the increase from one million to one billion which took twenty years. Beyond one billion, it becomes more difficult to project the future. Currently, the advances in nanotechnology has pushed the critical feature size down to around 22 nanometers, which approaches the physical limit of miniaturization [1].

While the individual integrated circuit (IC) components can be made smaller and

smaller so that more components can be packed onto a smaller area and, thus, increase the power of the chip, eventually there will be a point when the components can not be made any smaller and a more powerful next generation chip can not be created. This can be attributed to the fact that IC design over the last half-century or so has focused on only two dimensions. In essence, the IC has been constrained to designs that are essentially flat. A new design philosophy has emerged that incorporates a third dimension into IC design. These 3-D IC designs may hold the key to creating new, more powerful computers and electronic peripherals. These 3-D IC's consist of components that are stacked atop one another to create a three dimensional structure. This stacking of IC's possesses unique advantages such as the enhancement of device density per unit volume, the utilization of short vertical interconnects of improved electrical performance, and the capability of integrating multiple functions into a single package [2]. However, with this new design philosophy comes a new set of problems. These problems revolve around removing the heat from these densely packed chip stacks as well as aligning the electrical contacts within the chip stack itself, among others. Heat build-up within the chip stack can damage electronic components and will not be covered in this report. Improperly aligned chip stacks can introduce a residual shear force within the 3-D IC's which over time can induce failure of the electrical contacts. In addition, sudden shock caused by dropping the device can also create large shear forces on the electrical components. It is the effect of this shear force on the electrical contacts that will be examined in this report.

The idea behind 3-D IC's is fairly simple. Current 2-D IC's have gained performance by downscaling the size of the transistors on the chip in accordance with Moore's law. However, these transistors must be connected to all other components on the chip, such as power and memory, along planar paths. These planar paths create a resistive-capacitive, or RC, delay. When chip performance was relatively low, say 15 to 20 years ago, this RC-delay was not a major factor. However, as chips have

gotten faster due to the reduction in the size of the transistors, this interconnect RC delay has become a major source of circuit delays [3]. By stacking components into a chip stack containing all the necessary IC components, these paths can be shortened and, thus, the associated RC delay greatly reduced. The development of 3-D IC's is considered to be an enabling technology for the creation of smaller, more powerful, and more efficient electronic devices. Such devices would provide the advantages of a smaller form factor, higher performance, higher density integration, and lower power consumption, among other advantages.

As stated above, one of the problems in designing 3-D IC's involves the alignment of the electrical contacts, or solder joints. This solder joint alignment is likely to remain a limiting factor in the design rules for successful processing of 3-D IC's [4]. There exist many different methods for aligning solder joints. A common method involves optically using two 'alignment marks' on each wafer which are usually simple metal patterns produced along with the metal interconnects of the processed wafers that are to be aligned. Sub-micron across wafer alignment is possible using this method. In general, three methods are used to achieve alignment in 3-D integration and have been developed for micro-electro-mechanical system, or MEMS, processing. The first of these methods involves optical inspection and is limited to a transparent wafer and is non-destructive. The second method involves IR inspection and provides real-time reading of non-transparent silicon bonding and is also non-destructive. The third method utilizes a cross sectional destructive approach. This method is still at a research and development stage and involves techniques such as using an anisotropic etched silicon structure on the wafers to be aligned to obtain a type of keyed mechanical interlocking mechanism. This final method can produce self-alignment structures at the wafer surfaces that can improve the wafer-to-wafer alignment accuracy to well below one micron, even approaching 100 nm[3]. It should be noted that although a high degree of wafer-to-wafer alignment can be achieved for individual joints, in general, alignment will vary with position across a wafer stack. While some solder

joints and/or features might be well aligned, others may be less so.

As mentioned earlier, this misalignment can introduce a residual shear force within the 3-D IC and the greater the misalignment, the greater the residual shear force. A real breakthrough that was developed in the flip-chip electronic package industry was the introduction of underfill. This development gave solder interconnection technology an unforeseen mechanical robustness and a significant increase in flip chip solder joint fatigue resistance by reducing the inelastic strain sustained by the solder [5]. This report will examine the effect of underfill on a 3-D IC solder joint to see if there will be an equivalent increase in mechanical robustness in the solder joint with the presence of underfill. This underfill will be taken to be a polymeric material commonly used in the electronic package industry.

As plastic deformation is understood to be a kinetic process mainly controlled by the slip of dislocations [6], the material properties of the solder play an important role in the failure of the 3-D IC interconnect. Soldering can be defined as a process by which metals may be joined via a molten metallic adhesive (the solder) which on solidification forms strong bonds (usually intermetallic compounds) with the adherents and has been used since Roman times [7]. These intermetallic materials are brittle, may extend into the solder by needle-like growth or by detached fragments from the main body of the intermetallic, and are essentially thin layers of solder strained in shear. As such, the arrangement and size of the intermetallics may have a profound effect on overall solder joint behavior. Tin-based solders have been shown to have many useful properties such as relatively low cost, a conveniently low melting temperature, and excellent wetting characteristics with copper and brass [9]. Some common examples of intermetallics for eutectic solders on copper substrate are Cu_3Sn and Cu_6Sn_5.

Traditionally, soft solders are based on the tin-lead system. However, increasing concern about the safety of minute amounts of dissolved lead in drinking water has brought about the introduction and use of a range of lead-free solders. This event was spurred by the adoption of the Restriction of Hazardous Substances Directive

by the European Union. This directive prohibits the use of certain hazardous substances such as lead in electrical and electronic equipment being marketed after July 1, 2006 [8]. Recent studies into an acceptable lead-free solder has shown that solders containing silver gave the strongest joints [9]. In addition, a solder compound containing 98.5%Sn-1.0%Ag-0.1%Cu, also known as SAC101, was shown to have an absolute flow stress comparable to the 63Sn37Pb, a commonly used lead solder, and to be a good candidate for a lead-free replacement [10]. It is this solder that will be used in the numerical models employed in this study.

While these lead-free solder replacements are beneficial for the environment, they can result in an increased susceptibility of solder joint failure under drop conditions [11]. It is interesting to note that the solder joint in a piece of electronic equipment does not, in general, experience direct stress after impact. Rather, the mechanical shock induced by the impact will cause flexing in the printed circuit board, or PCB, and the solder joints will deform plastically in order to accommodate the imposed strain. On a typical PCB undergoing drop impact, the bulk of the solder joint will experience a strain rate of less than $1s^{-1}$. However, at the corners of the solder joint where failure will usually initiate, the strain rate can be above $200s^{-1}$ [10]. The strain rate imposed on the models in this study will fall between these two values.

In addition to the examination of the effects of solder joint thickness and the presence of underfill on the mode of failure in a solder joint, this report will also examine the effect of a periodic boundary condition, when performing finite element simulation, on the stress and strain fields within the model. During the research that was conducted for this paper, there were found to be many studies on the stress and strain fields within a solder joint. However, most of these experiments focused on a single solder joint and/or model. The effect of neighboring joints and/or models were not taken into account. This is significant because a solder joint is rarely, if ever, found as a single entity. Rather, it is part of a larger grid that is often periodic in structure. As such, any outside force, such as the flexing of the PCB caused by drop

impact, will have an effect on all parts of the whole. In addition, as all the solder joints are attached to the same PCB or two silicon substrates as in 3D packages, stresses and strains will be transferred from one joint into all of its neighbors. This report will examine the effect that this transference of stresses and strains has on the overall stress and strain fields in the first part of this research. The second part of this research will focus on the evolution of failure within a solder joint and how that evolution is affected by the presence of an underfill material.

Chapter 2

Numerical Model

The materials used in the model employed in this report are consistent with the materials that would be present in a stacked 3D IC. These materials are generally silicon, copper, an epoxy-based underfill material, and a tin-based lead-free solder. One of the major weaknesses in this type of modeling work is that the microstructure of the materials, such as copper, are ignored [4]. This microstructure influences many phenomenon including mechanical yield behavior. While accounting for the microstructure can be done by using methods such as a grain continuum approach to model the mechanics of polycrystalline materials as opposed to a purely continuum-based approach, these methods are computationally intensive. To alleviate the computational load, all materials used in the model are considered to be continuum-based. In addition, certain aspects of the model's structure, such as complex geometry, have been simplified in order to also reduce the computational time required since research has shown that doing so does not significantly affect the experimental results [12]. As such, the model consists of two silicon substrates with through-silicon-vias (TSV) made of copper that are connected using a lead-free solder joint, as shown in Figure 2.1. These copper TSVs have a landing pad on both the top and bottom for the lead-free solder joint. This study will examine a 5 micron, 10 micron, and 20 micron

solder joint thickness. It should be noted that although the copper TSV is stronger than the solder joint, it is not a rigid solid and will participate in the deformation process during loading [13]. For the test cases with the 20 micron-thick solder joint, the joint encompassed the entire area between the silicon substrates leaving no room for the copper TSV landing pad. The model was tested both with and without an epoxy underfill material. A drawing of the model is shown below.

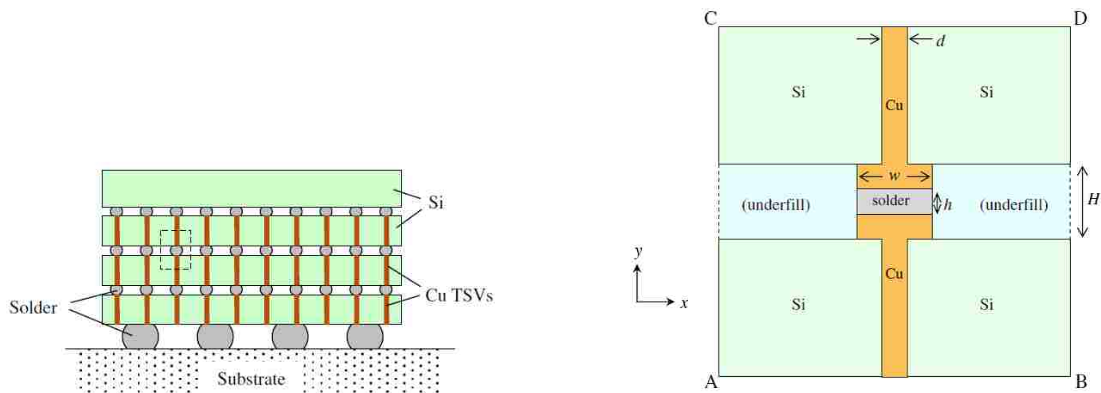

Figure 2.1: *Drawing of a 3D IC chip stack and a single interior solder joint. Symmetry is used to simplify the model.*

The experimental model was created using the FEA program Abaqus from Dassault Systems. Two modeling modes were used, static and dynamic. The static model utilized plane strain elements and was primarily used to investigate the effect of a periodic boundary condition on the stress and strain fields of the model when placed under a strain condition for varying solder joint thicknesses. The dynamic model also used plane strain elements and was used to investigate the mode of damage evolution and the pattern of fracture in the ductile solder joint for a solder joint thickness of 5 microns, 10 microns, and 20 microns when placed under similar strain conditions as the static model. These solder joint dimensions were chosen to reflect the current diameters employed by the electronic industry developed for 3D IC TSV microbump technology which are approximately 10 microns [1]. The model had an

overall height of 100 microns and an overall width of 100 microns. For comparison, all simulations were conducted both with and without an epoxy underfill. To simplify the simulations, only the lead-free solder Sn-1.0Ag-0.1Cu(SAC101)was examined and the creation of intermetallic compounds, such as Cu_6Sn_5, are ignored.

Table 2.1: Material Properties

Material Name	Youngs Modulus(MPa)	Poisson's Ratio	CTE	Density(kg/mm^3)
SAC101	47000	0.36	22.5E-6	5.76E-6
Silicon	130000	0.28	3.0E-6	2.33E-6
Copper	110000	0.30	17.0E-6	8.93E-6
Underfill	7000	0.33	32.0E-6	1.36E-6

Although the intermetallic layer has not been included in the models, it is a significant factor in the failure of a solder joint. The formation of an intermetallic is part of the soldering process. After the flux has removed the oxides and the solder has wetted the copper metallization, the flux starts dissolving into the molten solder and, after supersaturation, the molten solder immediately adjacent to the layer of copper starts forming solid Cu_6Sn_5 by heterogeneous nucleation [14]. Although other compounds will form, such as Cu_3Sn, Cu_6Sn_5 is the most stable phase in the Cu-Sn soldering reaction [15]. Research has shown that the presence of this intermetallic layer simply served to reduce the solder thickness while leaving all other deformation features within the solder in place [16]. As such, it is believed that its absence in this study does not significantly affect the results. Although it is not covered in this paper, the creation of intermetallic compounds at the interface of the solder joint with the copper TSV is significant with regard to the failure mode of the joint. This is due to the fact that an intermetallic compound, such as Cu_6Sn_5, is harder than the solder and is very well bonded to the copper TSV. This results in a predilection for crack formation at the interface of the solder and the intermetallic compound. This can be expedited by the creation of voids at the solder/intermetallic compound interface. The crack will propagate along the interface or through the voids during loading resulting in the eventual failure of the solder joint.

As stated above, two modeling modes were used. For both modes of loading, the models were constrained at the bottom nodes in the x and y directions. During the static loading mode, the top nodes of the models were subjected to a one-percent shear strain, or a ΔL of one micron. During dynamic loading, the top nodes of the models were subjected to a maximum shear strain of five-percent, or a ΔL of five microns, at a velocity of 0.05mm per second. This corresponds to an overall shear strain rate of $0.5s^{-1}$. It should be noted that although the dynamic model simulations were coded to a ΔL of five microns, all but one of the test cases experienced failure before this maximum displacement and the simulations were terminated before they were fully complete.

The first set of simulations examined the effect of a periodic boundary condition on the stress and strain fields of the model. This was done to gain insight into the effect that the strain of neighboring solder joints has on the solder joint in question. Nearly all of the numerical studies that focused on solder joint failure using FEA analysis with software such as ABAQUS or ANSYS focused on a single solder joint and did not take into account the effect of the neighboring joints. Logically, the strain and/or failure of solder joint would affect every joint surrounding it as all of the joints are attached to the same substrate. In the case of warpage induced by thermal mismatch, this gives rise to the concept of a critical solder joint, which can be thought of as the joint most likely to experience failure. Typically, this critical solder joint is located at the maximum Distance from Neutral Point (DNP) [17]. This neutral point can be thought of as the center of the electronic packaging. Additional studies have shown that it is the electronic board edge and, thus, the solder joints at the device edge that experience the maximum strain [18] under drop impact. The maximum strain experienced by these solder joints on the outer edges can be up to an order of magnitude higher than that experienced by solder joints that are closer to the neutral point [19]. However, the joints that are further away from the edge experienced strains that were fairly uniform in magnitude. It is these solder joints

located away from the edges of the package that are of interest for this study. As such, a boundary condition was included in the static models that would bind the nodes on the left edge to the corresponding nodes on the right edge. This boundary condition tied together their displacements in both the x and y directions. In this way, the model is constrained to transfer any displacement and, thus, loading along the edges to its neighboring solder joints and vice-versa. Simulations were also done both with and without this boundary condition for comparison.

In this study, the dynamic models were used to simulate failure within the solder joint. Previous work has shown that ductile failure under fast loading conditions occurs further away from the solder-intermetallic interface than it does during slower loading conditions [20]. As all of the models for used for the dynamic simulations did not include an intermetallic interface, encouraging failure within the solder itself, and not at the solder-intermettalic interface, was desirable. For these dynamic simulations, a progressive ductile damage model is utilized to simulate the failure of the solder joint. This damage process is quantified using a scalar damage parameter D, where the flow stress, σ, is defined as,

$$\sigma = (1 - D)\sigma_0, \tag{2.1}$$

where σ_0 is the flow stress in the absence of damage. D=0 corresponds to the absence of damage and a material element within the model will lose is capability to carry stress when the value of D attains unity. At this point, the element will be removed from the mesh in the model and a 'void' will be created. The cracking and eventual failure of the joint are then a consequence of linking multiple adjacent voids in the model. When damage is initiated, strain softening and, thus, strain localization set in. This process displays a strong mesh dependency and a characteristic length, L, is used to counteract this problem. This characteristic length is defined to be the square root of the integration point area in each finite element. The equivalent plastic strains correspond to ϵ_0^{pl} and ϵ_f^{pl} at the onset of damage (D=0) and failure

(D=1), respectively. In general, ϵ_0^{pl} can be made a function of the stress triaxiality, which is defined as the hydrostatic stress divided by the von Mises effective stress. Abaqus uses a plastic displacement quantity to quantify damage initiation. This is defined as,

$$u^p = L\epsilon^{pl} \tag{2.2}$$

where L is the characteristic length and ϵ^{pl} is the equivalent plastic strain. Prior to the onset of damage, $u^p = 0$. The failure and eventual removal of the material element will occur when u^p reaches a specified failure value, u_f^p. Going back to equation 2.1 for sigma, D can now be defined to be,

$$D = u^p / u_f^p \tag{2.3}$$

In this way, the damage response of the model can be completely specified by the two parameters, ϵ_0^{pl} and u_f^p. In the present study these values are chosen to be 0.18 and 0.000167, respectively. It should be noted that the value chosen for u_f^p corresponds to a ϵ_f^{pl} value of 0.5 which was based on measured tensile stress-strain curves of bulk pure Sn or Sn-rich solder alloy [21]. More information on this damage initiation process can be found in the ABAQUS Users Manual.

The simulation of failure using ABAQUS gains validity when viewed with respect to actual experiments. Laboratory experiments have shown that solder joint failure often occurs entirely within the solder outside of the intermetallic layer [6]. With regard to the method of simulating the removal of material elements and eventual failure of the joint, studies would suggest that the dominant strain parameter is the equivalent strain calculated from the von Mises criterion [7]. In addition, although it has been suggested that the hydrostatic component of stress does not affect plastic yielding [6], when failure criteria are put in terms of stress triaxiality, which is hydrostatic stress divided by von Mises effective stress, it can be argued that hydrostatic

stress does indeed play a role in the failure of a solder joint, if indirectly. Finally, general failure criteria for physical laboratory experiments include the onset of a visible crack and the start or a given percentage fall in stress as seen in a load-displacement curve. These same criteria are used for these simulations.

Chapter 3

Results: Periodic vs. Non-Periodic Boundary Condition

Previous models used to investigate the effects of shear on solder joint integrity have used boundary conditions that were not periodic with respect to the overall 3D IC structure. For example, while the model under investigation itself is considered to be a unit cell construct of the entire planar view of the 3D IC, the previous models did not reflect boundary conditions that could accurately model this. These boundary conditions did not take into account the effect of the neighboring unit cells, also undergoing shear, and how they would affect the stress and strain fields of the model under investigation. To remedy this, a boundary condition was added that would tie the x and y displacement of the nodes on the left side of the model with the corresponding node along the x-axis, with the same y-coordinate, on the right side of the model. In this way, the effect of the shearing force that would be felt by the adjacent unit cells can be simulated to be displacing the edge nodes of the model under investigation thereby affecting its stress and strain fields. This will allow the model to be a more accurate representation of a single unit cell of the entire body, as opposed to a single, stand-alone module. For these simulations investigating the

effect of a periodic boundary condition, a static model was used that did not model failure of the solder joint. The reason for this will be discussed at the end of this section.

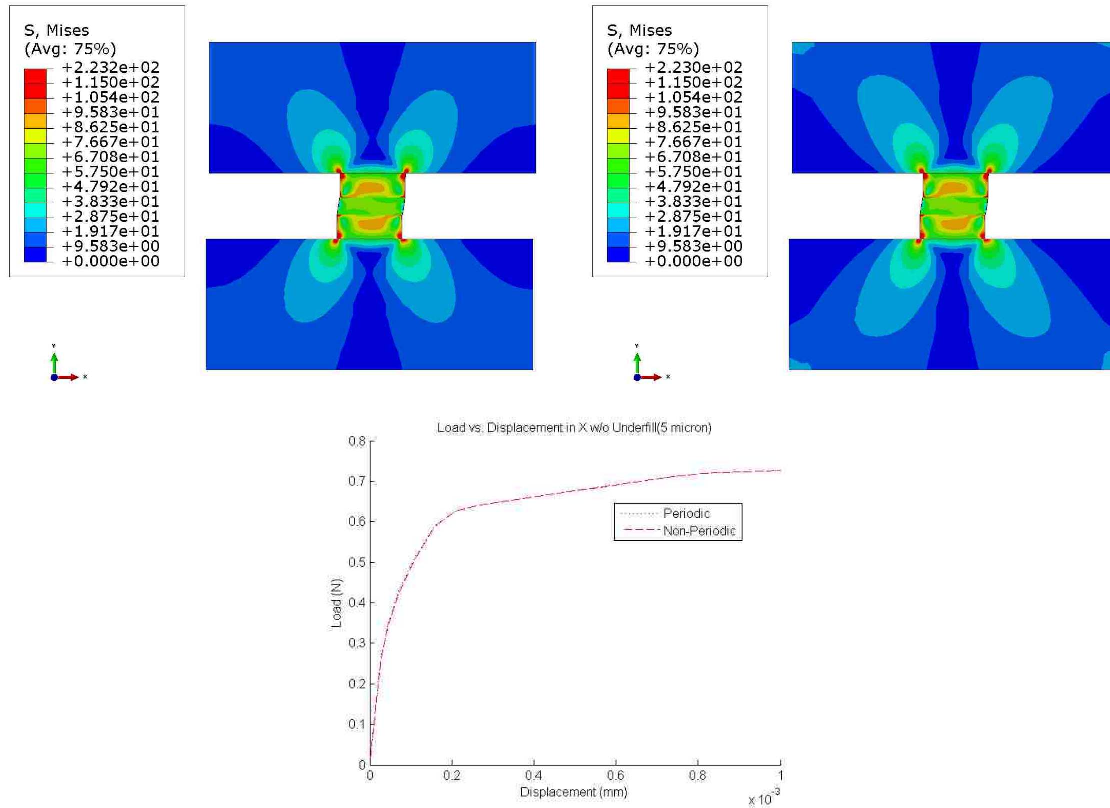

Figure 3.1: *Abaqus model showing von Mises stress without underfill present for a 5 micron solder joint with periodic B/C on the left and non-periodic B/C on the right. A plot of load versus displacement is included for comparison.*

The effect of introducing this periodic boundary condition produced mixed results. For the models without underfill, the results for the periodic models are virtually indistinguishable from the results of the non-periodic model. As can be seen in the figures 3-1 to 3-6,the Von-Mises stress field is nearly identical for all models with and without a periodic boundary condition for each solder thickness. The same is also true of for the equivalent plastic strain field and the shear stress field for these

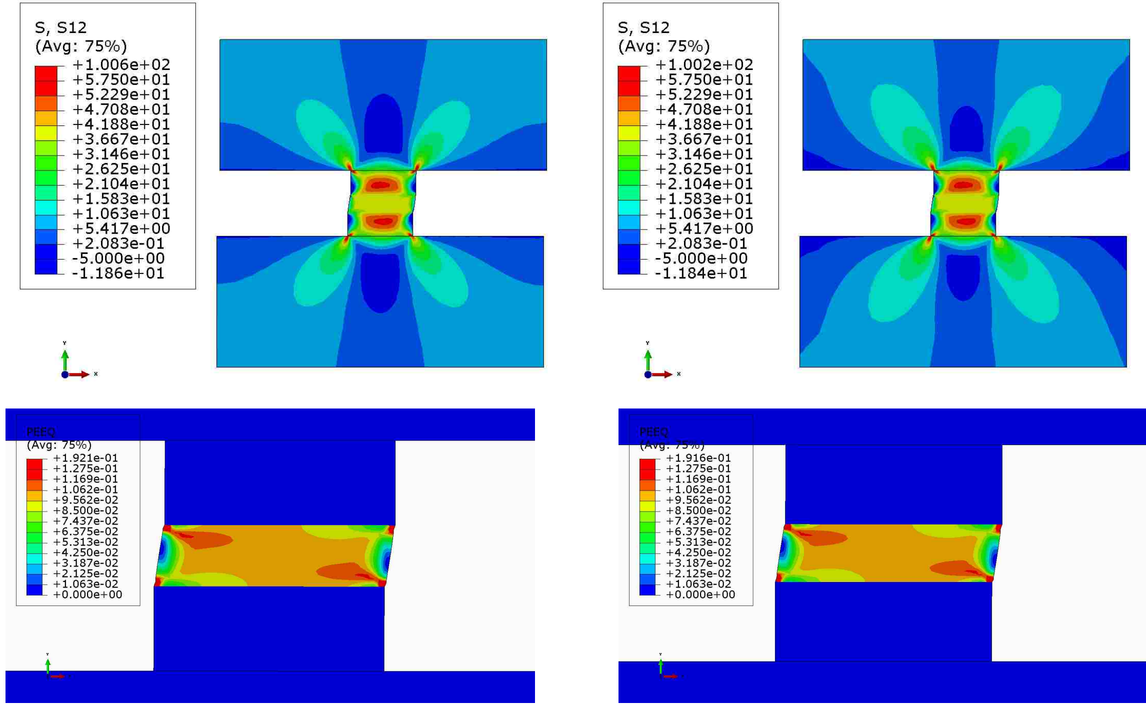

Figure 3.2: *Abaqus models showing shear stress and equivalent plastic strain without underfill present for a 5 micron solder joint. The models with the periodic boundary condition are on the left and the non-periodic boundary condition models are on the right.*

models. Plots of load versus displacement in the x direction for each solder thickness of all cases without underfill are displayed together for comparison.

Beginning with the 5 micron solder joint without underfill present, it can be seen in Figure 3.1 that the von Mises stress field for the model with the periodic boundary condition is nearly identical to the model without the periodic boundary condition. The largest difference in the von Mises stress comes at the corners of the models. The model without the periodic boundary condition displays pockets of stress at the four outside corners of the model. This is unrealistic when viewed in terms of the complete 3D IC package. The model with the periodic boundary condition displays a much more uniform von Mises stress field, particularly at the boundaries. However, despite minor differences, both the model with the periodic boundary condition

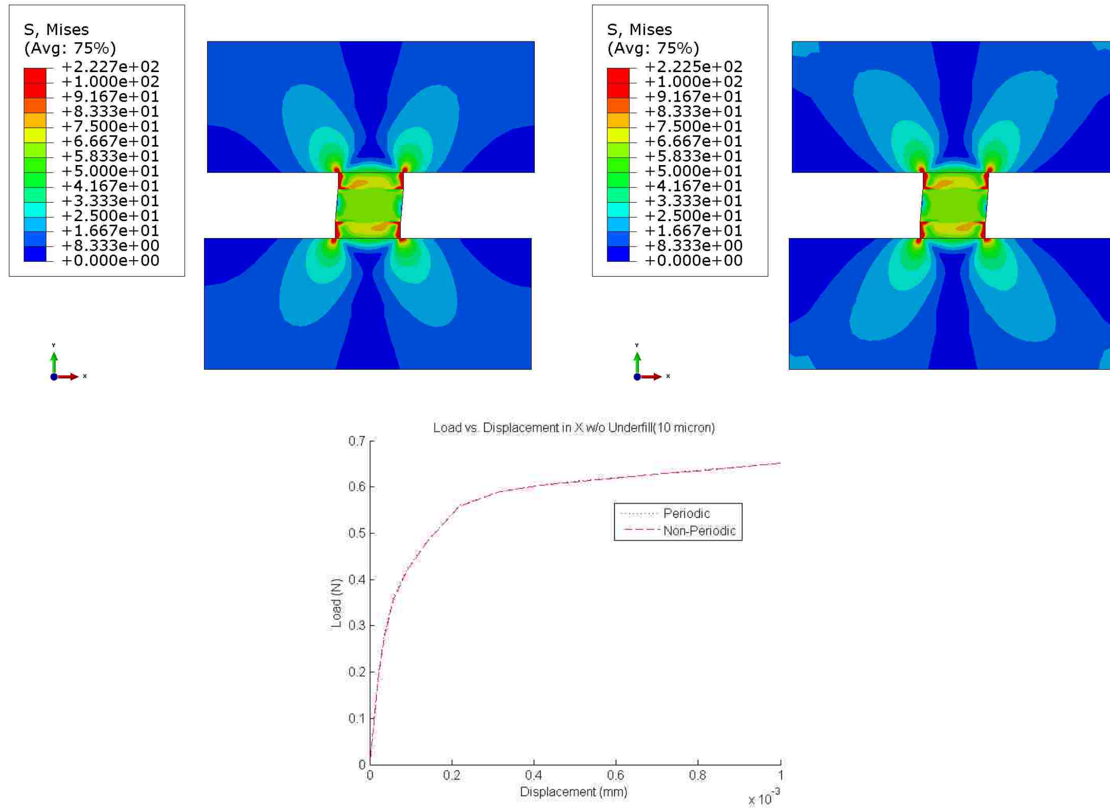

Figure 3.3: *Abaqus model showing von Mises stress without underfill present for a 10 micron solder joint with periodic B/C on the left and non-periodic B/C on the right. A plot of load versus displacement is included for comparison.*

and the model without it display very similar load responses. This is evident in the fact that the plots of load versus displacement for both models fall on top of each other. As can be seen in Figure 3.2, the shear stress and equivalent plastic strain fields for the models with and without the periodic boundary condition are also very similar to each other. The greatest difference can be seen in the shear stress field surrounding the copper TSV. The shear stress field for the model with the periodic boundary condition is larger and extends further into the silicon substrate than the model without the periodic boundary condition. The equivalent plastic strain fields for both models are virtually identical.

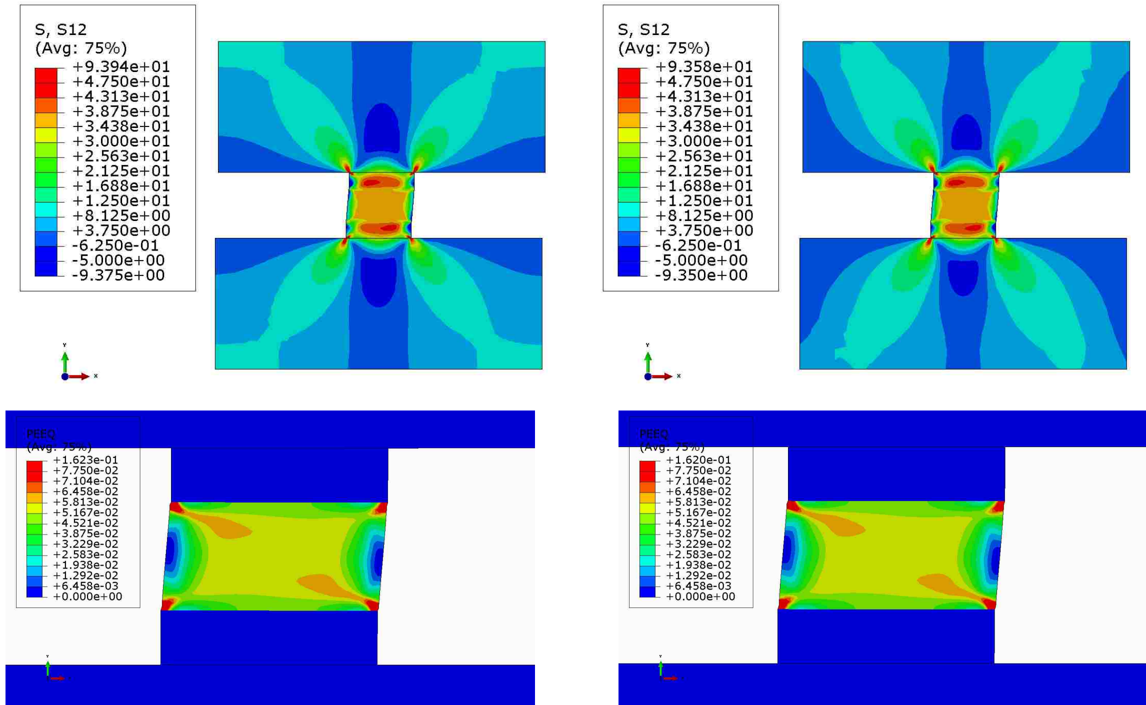

Figure 3.4: *Abaqus models showing shear stress and equivalent plastic strain without underfill present for a 10 micron solder joint. The models with the periodic boundary condition are on the left and the non-periodic boundary condition models are on the right.*

Moving on to the 10 micron solder joint without underfill present, from Figure 3.3 it can be seen that the von Mises stress field for both models is also very similar. Once again, the greatest difference between the model with a periodic boundary condition and the model without one is the pockets of stress at the corners of the model without the boundary condition. Both models also display very similar load responses. This is seen in the plots for load versus displacement, which fall on top of each other for both models. As seen in Figure 3.4, the shear stress and equivalent plastic strain fields for both models also show very similar features. As with the previous model, the largest difference can be seen in the shear stress field surrounding the copper TSV which is also larger and extends further into the silicon substrate while the equivalent plastic strain fields for both models are again virtually identical.

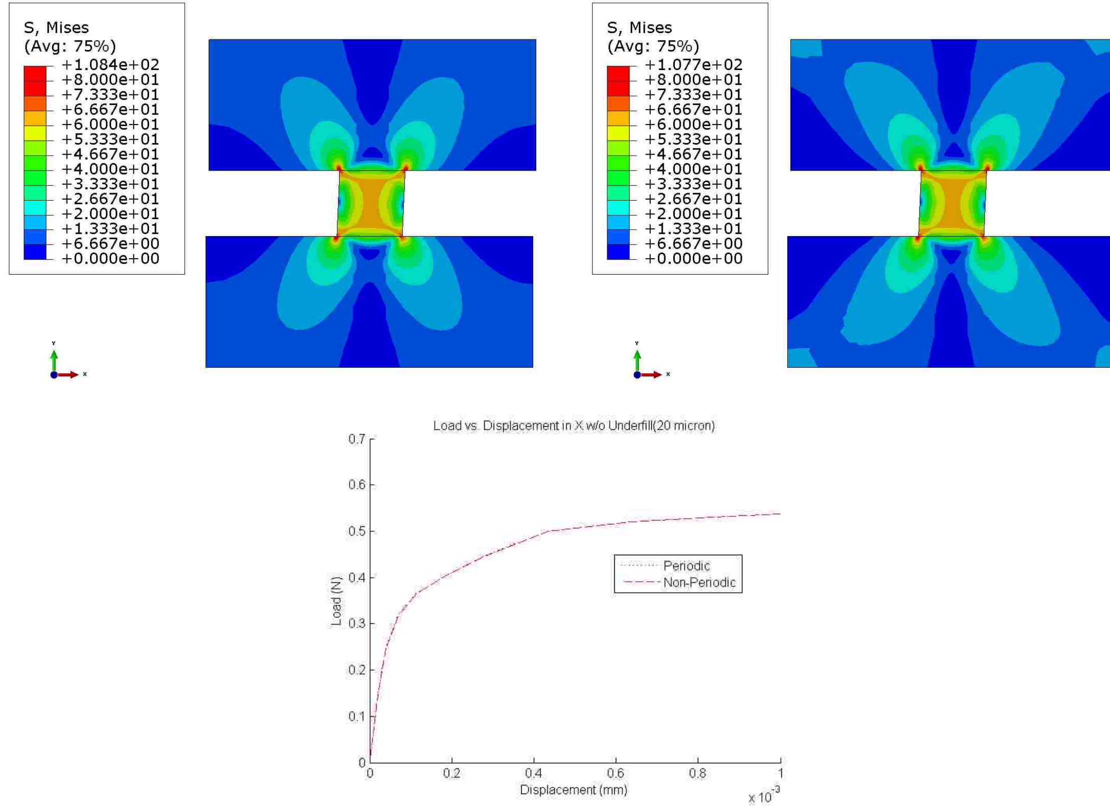

Figure 3.5: *Abaqus model showing Mises stress without underfill for a 20 micron solder joint with periodic B/C on the left and non-periodic B/C on the right. A plot of load versus displacement is included for comparison.*

For the 20 micron solder joint without underfill present, there are no substantial deviations from the results seen in the previous two solder thicknesses without underfill. As with the 5 and 10 micron solder joints, Figure 3.5 shows that the von Mises stress fields for both the model with a periodic boundary condition and the model without a periodic condition are very similar save for the stress concentrations in the corners of the model without the boundary condition. Once again, the plots of load versus displacement for both models fall on top of each other indicating a similar load response from both models. Figure 3.6 shows that the shear stress and equivalent plastic strain fields are very similar, as well. However, where the corners

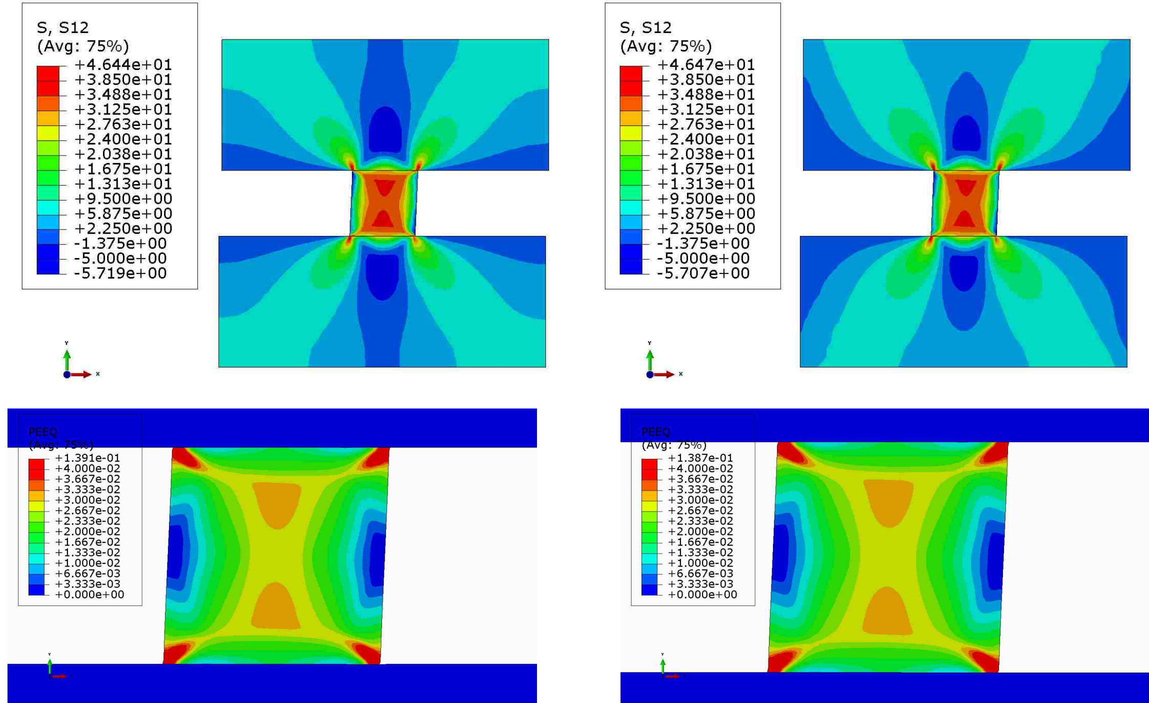

Figure 3.6: *Abaqus models showing shear stress and equivalent plastic strain without underfill present for a 20 micron solder joint. The models with the periodic boundary condition are on the left and the non-periodic boundary condition models are on the right.*

of the 5 and 10 micron solder thickness models displayed stress concentrations at the corners of the model, the 20 micron solder thickness model displays no such features. The shear stress field for the model with the periodic boundary condition is more symmetric along the 45 degree preferred shear path. As with the previous two test cases, the equivalent plastic strain fields are virtually indistinguishable from each other.

All of the test cases for models without underfill present show very similar features both with and without the periodic boundary condition in nearly all of the stress and strain fields. Von Mises and shear stress fields display only minor differences in all of the test cases without underfill present. This similar load response is confirmed in the plots of load versus displacent, which are identical for load cases with and without

the periodic boundary condition. In addition, the equivalent plastic strain fields for the test cases with the periodic boundary condition are virtually indistinguishable from the test cases without the boundary condition. For these reasons, it can be assumed that the effect of transferred shear from adjacent unit cells has little or no effect on the stress and strain fields of the model under investigation when there is no underfill present.

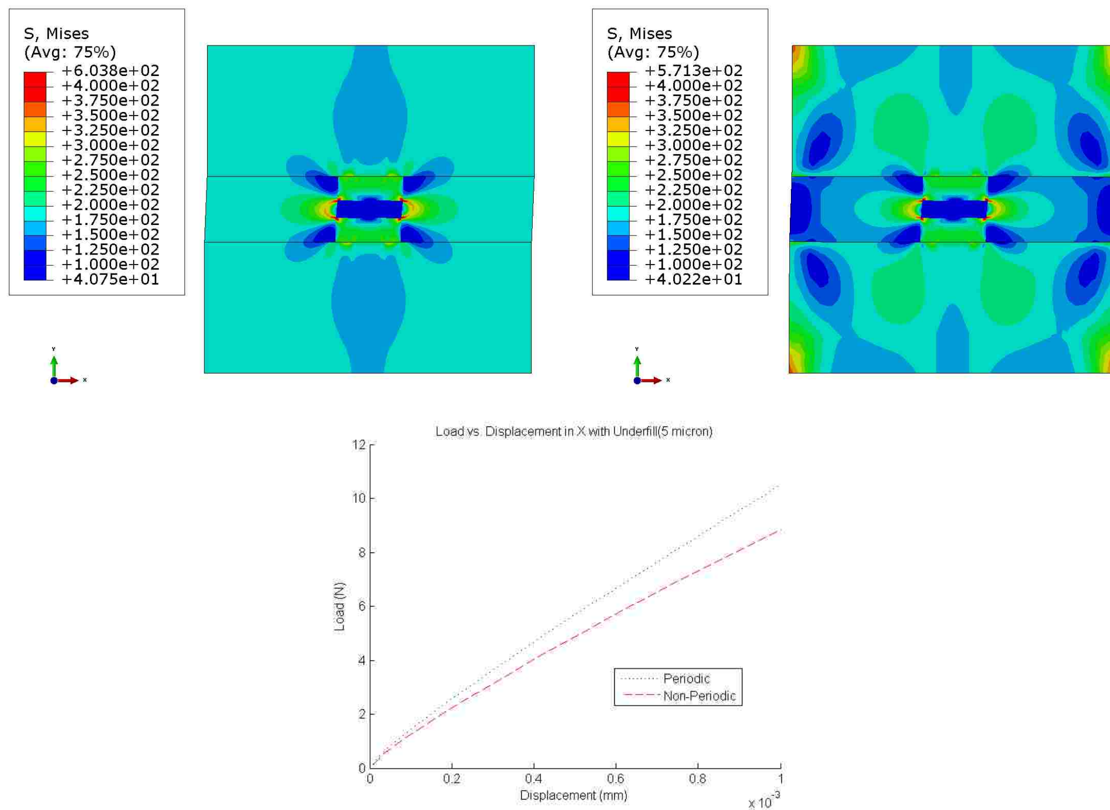

Figure 3.7: *Abaqus model showing Mises stress with underfill present for a 5 micron solder joint with periodic B/C on the left and non-periodic B/C on the right. A plot of load versus displacement is included for comparison.*

However, for the models with underfill, the difference is dramatic. The stress and strain fields of the models with the periodic boundary condition are very different from the stress and strain fields of the models without the periodic boundary con-

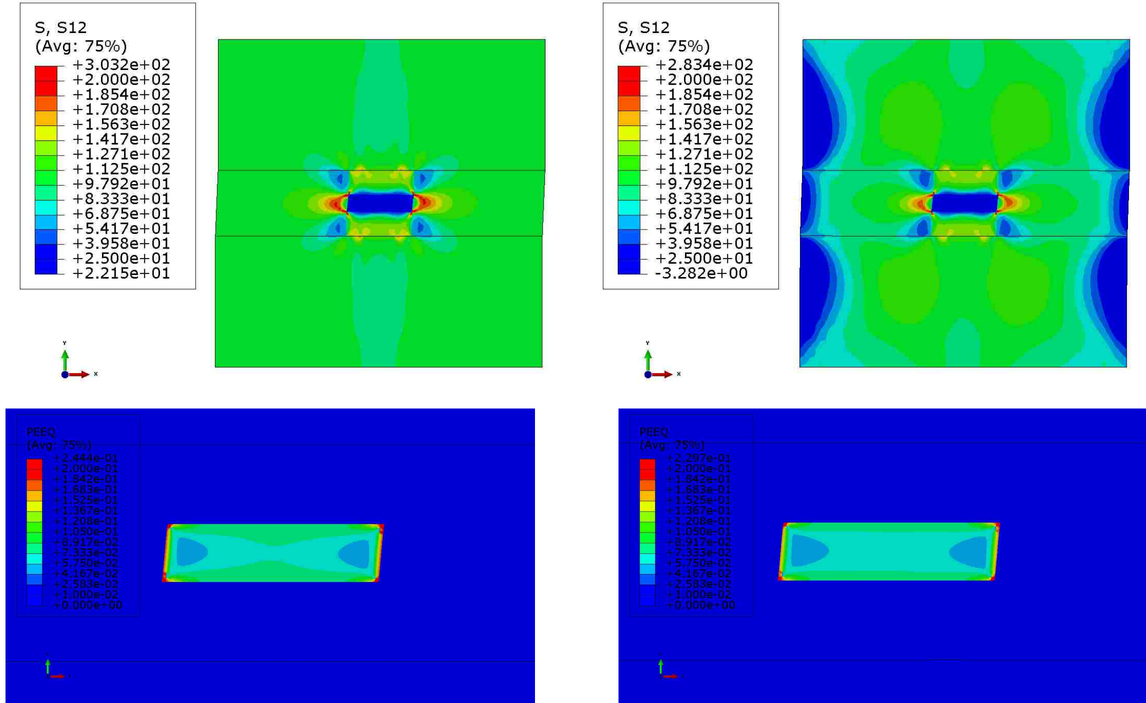

Figure 3.8: *Abaqus models showing shear stress and equivalent plastic strain with underfill present for a 5 micron solder joint. The models with the periodic boundary condition are on the left and the non-periodic boundary condition models are on the right.*

dition. As can be seen from the figures 3.7 to 3.12, the stress fields of the periodic models are much more uniform than the stress fields of the non-periodic models. This is especially true around the left and right edges of the models where the non-periodic models display pockets of lower stress that appear within the strata of the silicon and are also concentrated on the edges of the underfill material. The periodic models show no such pockets or concentrations of lower stress around the left and right edges of the structure but do show a more uniform concentration of stress within and around the TSV. Plots of load versus displacement in the x direction for each solder thickness both with and without the periodic boundary condition are displayed together for comparison.

Considering the 5 micron solder joint with underfill present, it can immediately be

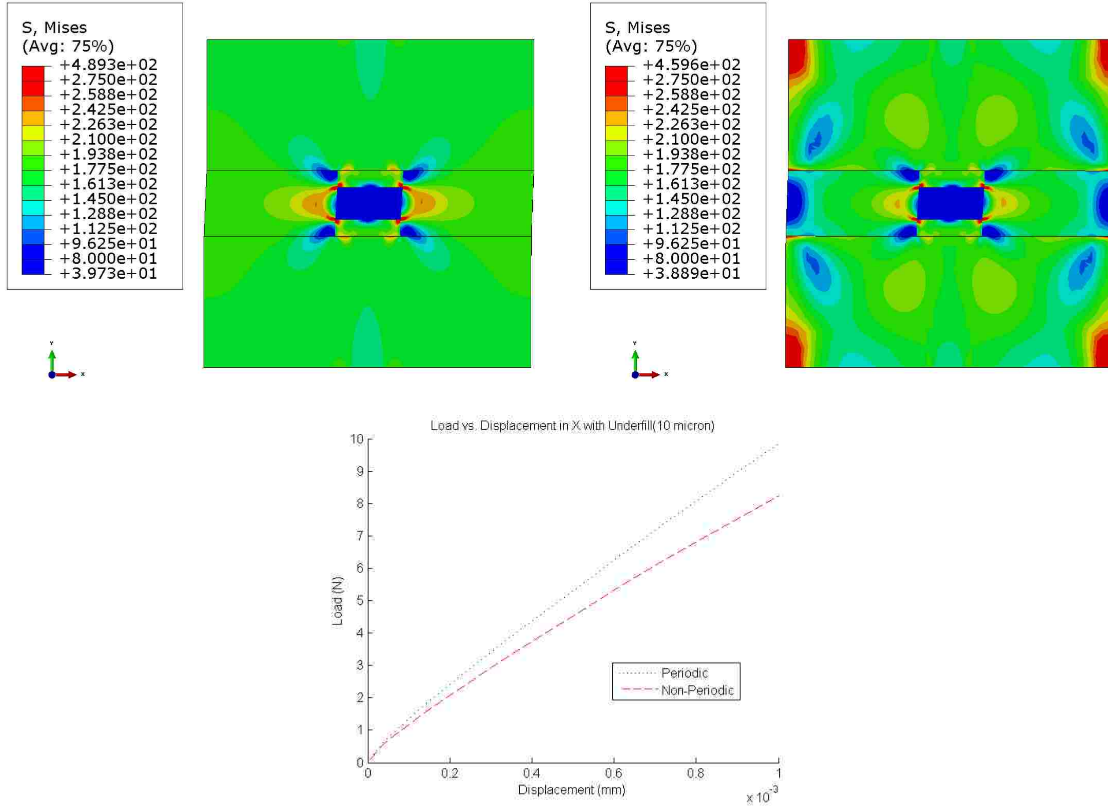

Figure 3.9: *Abaqus model showing von Mises stress with underfill present for 10 micron solder joint with periodic B/C above and non-periodic B/C below. A plot of load versus displacement is included for comparison.*

seen in Figure 3.7 that there is a dramatic difference in load response when there is a periodic boundary condition present. The von Mises stress field for the model with the periodic boundary condition is very uniform in the underfill material and silicon substrate. For the model without the boundary condition, although the von Mises stress field is symmetrical about the copper TSV, there are a large number of stress irregularities throughout the model. There are also the same stress concentrations at the corners of the model that were present in the 5 micron model without underfill. Less of the von Mises stress seems to be concentrated in the copper TSV for the model with the periodic boundary condition than in the model without it. The plots

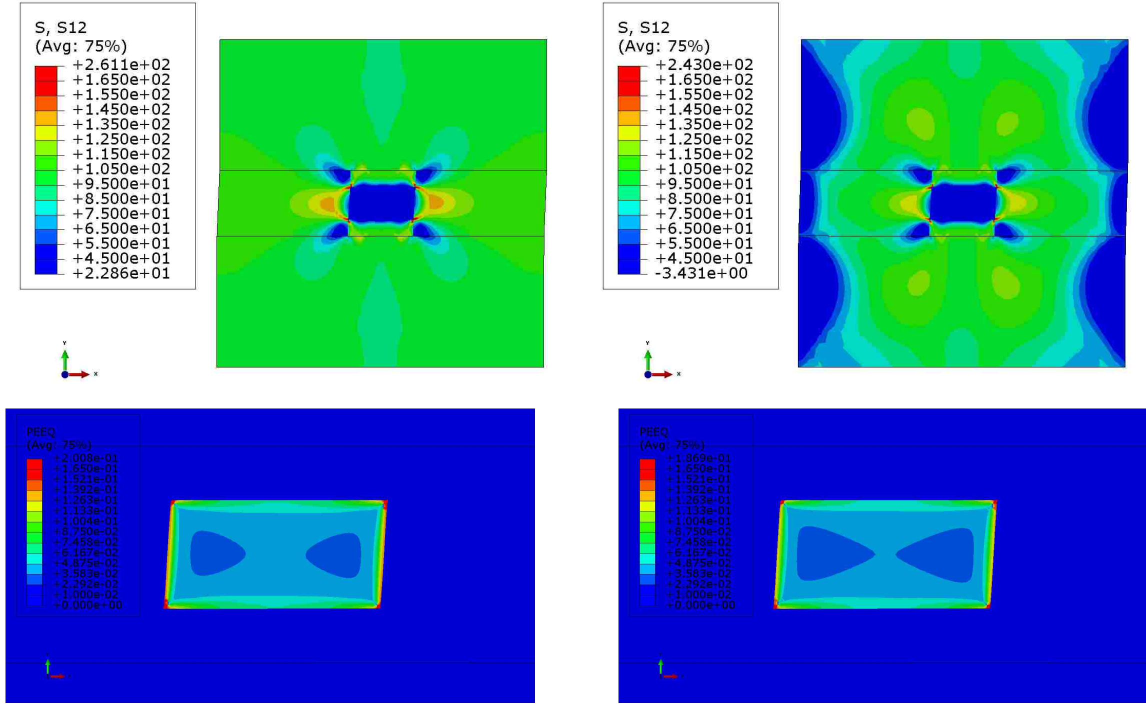

Figure 3.10: *Abaqus models showing shear stress and equivalent plastic strain with underfill present for a 10 micron solder joint. The models with the periodic boundary condition are on the left and the non-periodic boundary condition models are on the right.*

of load versus displacement show that the model with the periodic boundary condition requires a higher loading for the same amount of displacement than the model without the boundary condition. Figure 3.8 shows that the shear stress fields also highlight the dramatic difference in load response when there is a periodic boundary condition present. As with von Mises stress, the shear stress field for the model with the periodic boundary condition is very uniform in the underfill material and silicon substrate compared to the model without the boundary condition. The equivalent plastic strain fields show a higher plastic strain in the model with a periodic boundary condition, particularly along the solder joint interfaces.

The 10 micron solder joint with underfill present displays results similar to the 5 micron joint. Figure 3.9 shows that the von Mises stress field for the model with the

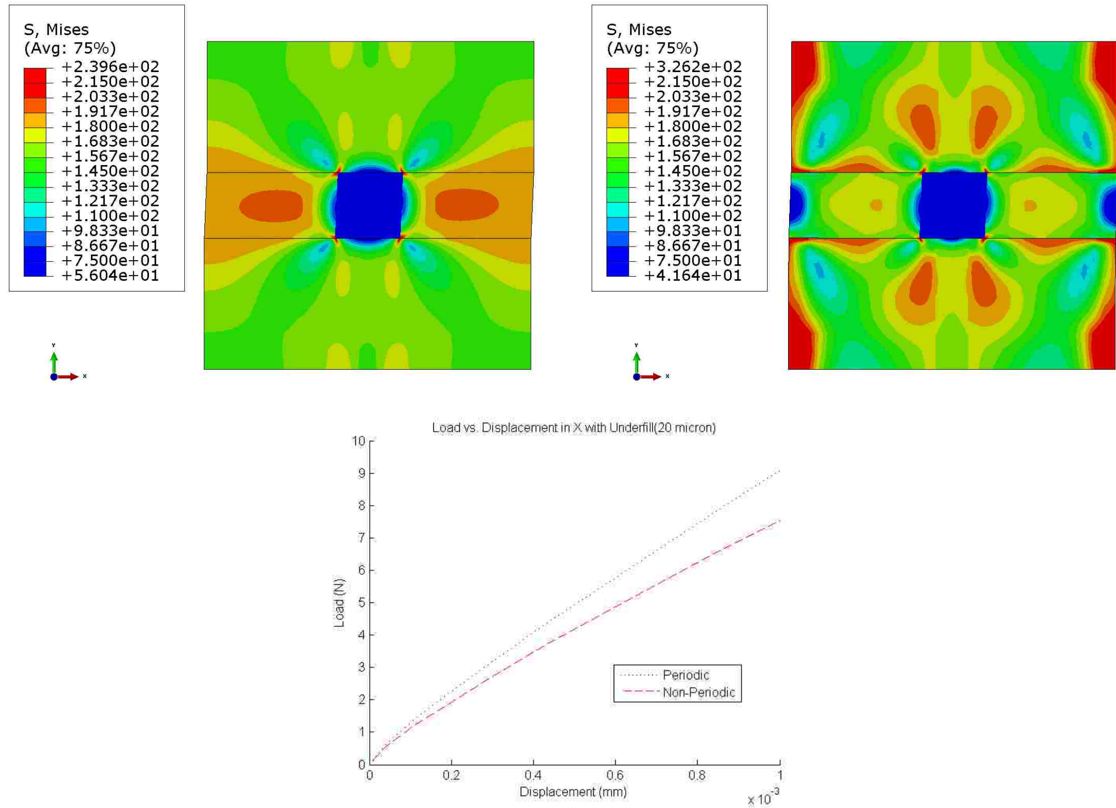

Figure 3.11: *Abaqus model showing von Mises stress with underfill present for 20 micron solder joint with periodic B/C on the left and non-periodic B/C on the right. A plot of load versus displacement is included for comparison.*

periodic boundary condition is much more uniform throughout the underfill material and silicon substrate than the model without the boundary condition. In addition to the model without the boundary condition displaying large von Mises stress concentrations at the corners of the model, it also displays large stress concentrations at the interface of the underfill material and the silicon substrate. As with the previous test case with underfill present, the load versus displacement plots also indicate that the model with the periodic boundary condition requires a higher loading for the same amount of displacement than the model without the boundary condition. As seen in Figure 3.10, the shear stress fields continue to demonstrate the dramatic difference in

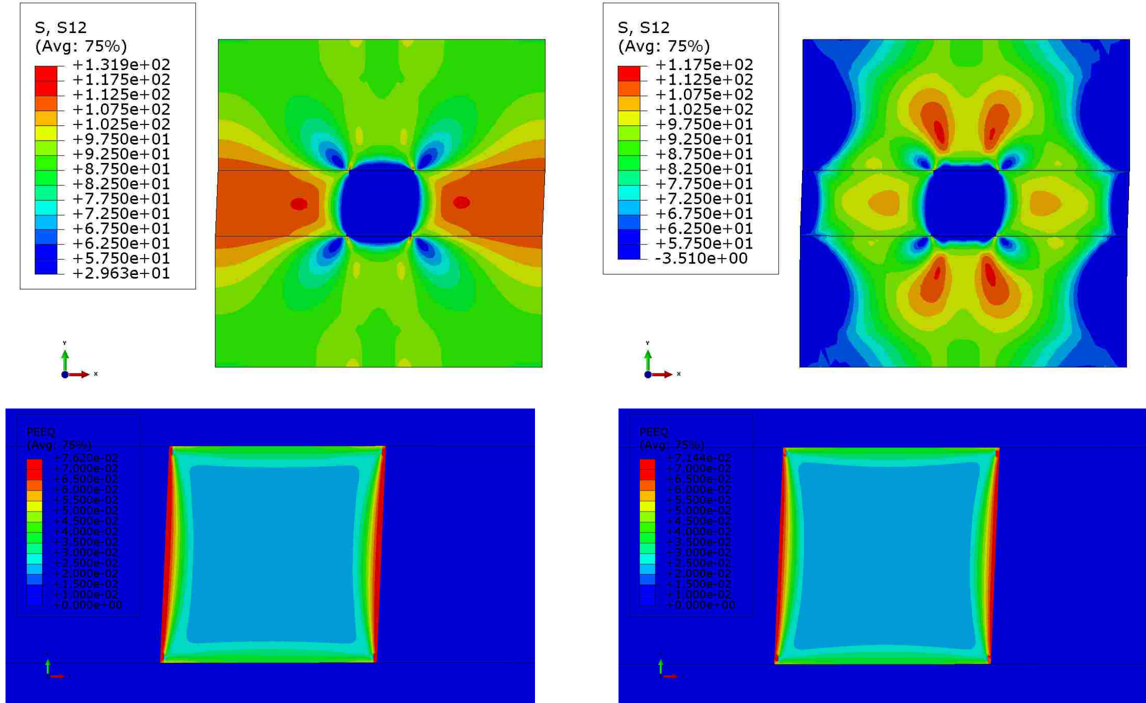

Figure 3.12: *Abaqus models showing shear stress and equivalent plastic strain with underfill present for a 20 micron solder joint. The models with the periodic boundary condition are on the left and the non-periodic boundary condition models are on the right.*

load response for a model with a periodic boundary condition. The shear stress field for the model with the boundary condition is once again very uniform throughout the silicon substrate compared to the model without it and shows a higher shear stress in the underfill material that is transferred into the silicon substrate along the underfill/substrate interface. Comparing the equivalent plastic strain fields for both models shows that the model with the periodic boundary condition also displays a higher plastic strain along the solder joint interfaces.

The 20 micron solder joint with underfill present displays results that are similar to the previous two test cases with underfill present. As with the previous two cases, Figure 3.11 shows that the von Mises stress fields for both models are dramatically different. While the von Mises stress field for the model with the periodic bound-

ary condition is not as uniform as the previous cases, it displays none of the stress concentrations at the corners of the model or along the underfill/substrate interfaces that are present in the model without the boundary condition. Once again, there is less von Mises stress present around the copper TSV and more von Mises stress present in the underfill material in the model with the periodic boundary condition. The load versus displacement plot also indicates that the model with the boundary condition requires more loading for the same amount of displacement than the model without the boundary condition. Similar to the 10 micron joint with underfill present, Figure 3.12 shows that the shear stress field for the model with the periodic boundary condition displays higher shear stress in the underfill material that is transferred along the underfill/substrate interface into the silicon substrate and the area around the copper TSV seems to experience less shear. The equivalent plastic strain fields also seem to indicate that there is higher plastic strain along the solder interfaces in the model with the boundary condition.

For the test cases with underfill present, while the deformation appears to be approximately the same, there can be approximately 20 percent higher force required for the same amount of deformation in the material for the models that have the periodic boundary condition present. In addition, the von Mises and shear stress fields are dramatically different for test cases with the boundary condition when underfill is present. The equivalent plastic strain also appears to be higher at the solder joint interfaces for test cases with underfill and a periodic boundary condition. For these reasons, it can be assumed that the effect of shear from adjacent unit cells has a large effect on the stress and strain fields of the model under investigation when there is underfill present. It is interesting to note that examination of the equivalent plastic strain fields for all of the test cases with underfill present reveals that regions of high plastic strain develop along the solder joint/underfill interface prior to developing within the bulk solder. This becomes a significant factor in the results of the second part of this research.

As was stated earlier in this section, a static model was used to investigate the effect of a periodic boundary condition that did not simulate the failure of the solder joint. The reason for this has to do with the complexity of modeling the effect of the failure of a solder joint on the stress and strain fields of the adjacent solder joints. If it can be assumed that all joints will fail together at the same time, then the concept of using a single unit cell structure to model the behavior of the entire 3D IC is valid. However, it is not realistic to assume that all solder joints will fail at exactly the same time. It is more realistic to assume that microscopic defects within the structure and/or slight imperfections in the manufacture of the 3D IC will lead to stress concentrations within certain solder joints causing these joints to fail first. In the case of no underfill, these initial failures will lead to stress being transferred through the silicon into the adjacent solder joints where a build-up of stress may lead to the failure of the joint. If it does lead to failure, stresses are again transferred through the silicon into the adjacent solder joints propagating the chance of joint failure throughout the matrix. Since it is possible for two joints that are not adjacent to one another to fail at approximately the same time, it becomes more and more difficult to model the behavior of the entire structure under a shearing condition. It should be noted that these same defects within the silicon and/or imperfections in manufacture can result in a slightly stronger solder joint that is capable of withstanding higher levels of shear stress before failing. If underfill is considered, the situation becomes even further complicated. The underfill material can act as either an impediment or a catalyst to joint failure depending on the condition of the bonding to the joint and the material properties of the underfill. It is also worth mentioning that the effects of the unit cells above and below the solder joint in question will also have an effect on the stress and strain fields on the unit cell between them. For all of these reasons, modeling the behavior of the overall 3D IC structure becomes even more problematic. As a result, modeling with any degree of fidelity the failure of individual solder joints, and their effect on adjacent solder joints, becomes a computationally intensive

endeavor.

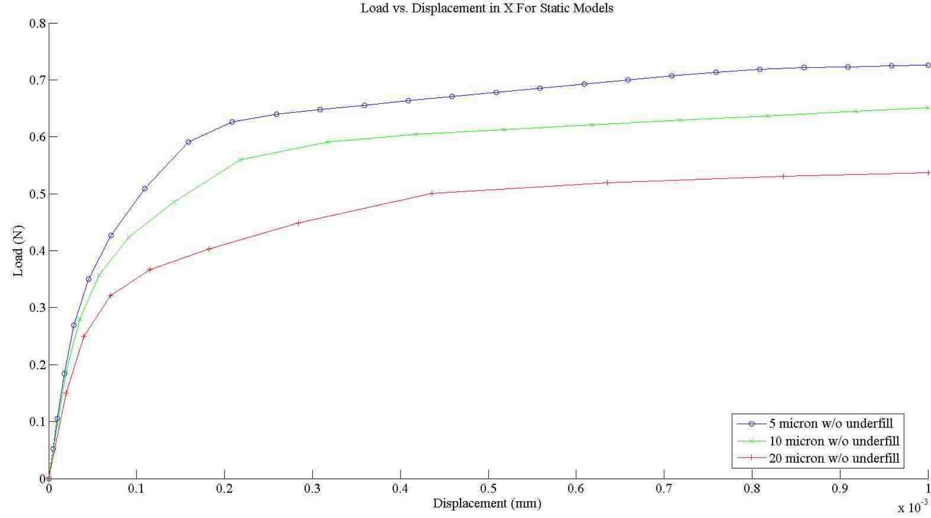

Figure 3.13: *Plots of load versus displacement for the test cases without underfill present for the test cases that included a periodic boundary condition. Note that although the 5 micron solder joint is able to resist a higher loading than the 10 or 20 micron joints.*

Overall, including a periodic boundary condition in the numerical model produced results that are qualitatively similar to the results of the study undertaken in Ref. 2 [Shen & Johnson]. The study by Shen & Johnson was done with a similar numerical model that did not include a periodic boundary condition and concluded that "a thinner solder layer (solder joint) sandwiched between copper pads displays a better mechanical resistance to overall shear". Shen & Johnson also concluded that "(t)he existence of underfill significantly raises the shear force required to attain a given overall shear displacement". Similar conclusions can be drawn from the examination of Figures 3.13 and 3.14. These plots of load versus displacement highlight the fact that the 5 micron solder joint is able to resist a higher loading whether there is underfill material present or not. In addition, the load axis on the plot for the test cases that contain underfill material (Figure 3.14) is an order of magnitude greater

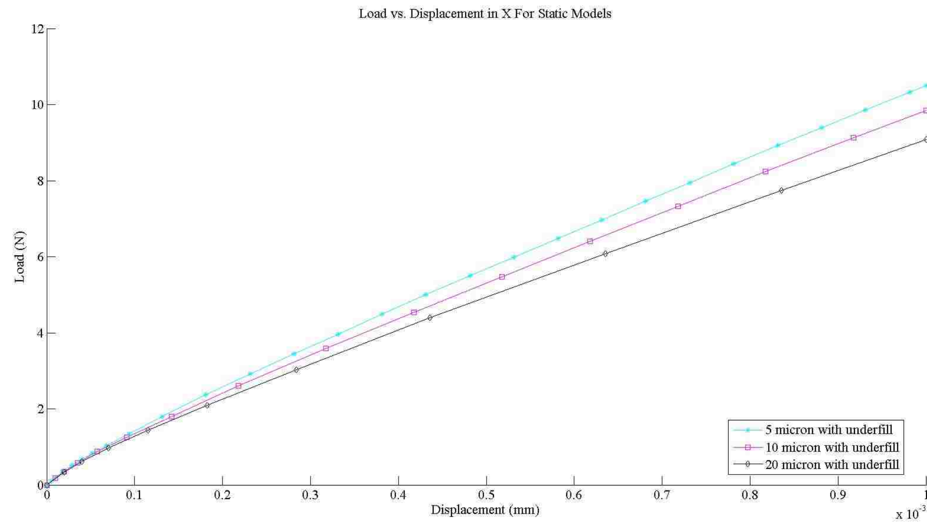

Figure 3.14: *Plots of load versus displacement for the test cases with underfill present for the test cases that included a periodic boundary condition. Note that the 5 micron solder joint is able to resist a higher loading than the 10 or 20 micron joints.*

than the load axis on the plot for the test cases that do not contain underfill material (Figure 3.13) implying that underfill material does indeed produce a stronger joint. It is interesting to note that the previous study also observed the localization of plastic strain along the solder joint/underfill interface, which was seen in all of the current test cases with underfill material present whether a periodic boundary condition was included or not. This implies that the risk of damage around the solder joint/underfill interface is a valid concern when using underfill material in 3D IC packages.

Chapter 4

Results: Solder Joint Fracture and Mode of Failure

This second part of this research focused on the evolution of damage and eventual failure of the solder joint under a strain condition. Much like the first part of this research, three different solder joint thicknesses were used- 5 micron, 10 micron, and 20 micron. In addition, each solder joint thickness was simulated with and without underfill in order to examine the effect of underfill material on the damage evolution. The solder joints were subjected to a maximum shear displacement of 5 microns, or 5% nominal shear strain, in the positive x-direction. Plots of load versus displacement are also provided for each test case. It should be noted that nearly all of the solder joints experienced failure before the maximum strain was reached and that the simulations were terminated prior to completion for these joints. The one exception was the 20 micron joint with underfill present which, although completely delaminated from the underfill, had not yet experienced failure in the bulk solder. More on this results will be discussed later in this section.

Previous work in this area has concluded that maximum strains will be located at the solder joint to TSV interface [22]. In addition, the failure or crack propagation will

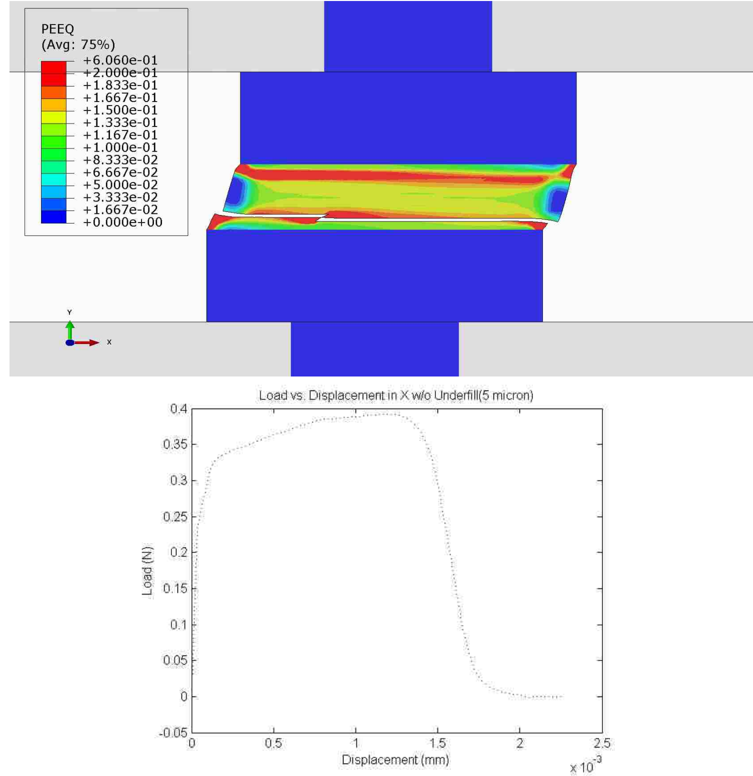

Figure 4.1: *Abaqus model showing the failure of the 5 micron solder joint without underfill present. The load versus displacement curve showing the significant drop in loading at approximately 1.5 microns indicates that the joint has failed.*

follow the path of greatest equivalent plastic strain [20]. For this reason, equivalent plastic strain has been used to display failure progression in the ABAQUS models. In a physical solder joint without underfill present, as opposed to a simulated one, the exact cracking feature can depend on the local microstructure. However, the macroscopic failure path is largely limited by the well developed plastic band parallel to the interface. The evolution of this band involves several steps. Initially, strong plasticity appears in the four corner regions under a horizontal strain condition and will tend to propagate into the solder along an approximate 45 degree direction. But, because the dominant deformation mode is horizontal shear, linking of the plastic localization initiating from the two interface corners tends to occur. This results

in a band parallel to each solder joint/TSV interface [16]. The continual strain of this plasticity band will eventually generate voids. These voids can be generated in the intermetallic layer from the over-consumption of Cu atoms [23], or from the separation of grain boundaries within the solder material. The linking of these voids will result in the eventual failure of the solder joint.

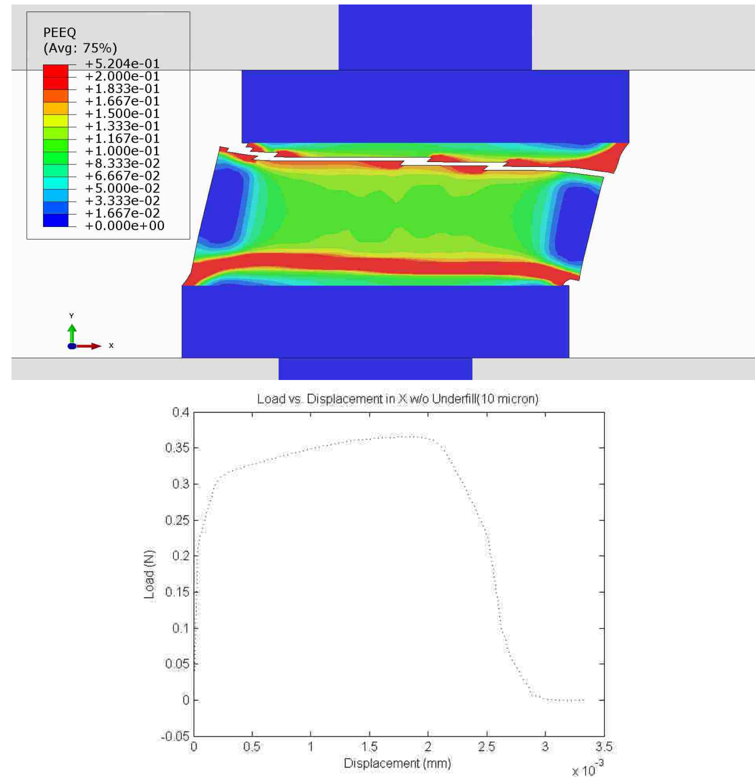

Figure 4.2: *Abaqus model showing the failure of the 10 micron solder joint without underfill present. The load versus displacement curve showing the significant drop in loading at approximately 2.5 microns indicates that the joint has failed.*

The ABAQUS modeling appears to have verified these observations, particularly in the cases without underfill present. As can be seen in figures 4.1 to 4.3, these cases seem to corrolate well with the results of previous research and are examined first. As the simulations for these test cases progresses, a strong band of plasticity develops that is parallel to the solder joint/TSV interface. It is along this band of plasticity

that failure occurs for all test cases without underfill present.

The 5 micron solder joint without underfill present is examined first. Examination of Figure 4.1 shows that, as expected, areas of high equivalent plastic strain begin to develop at the corners of the solder joint as the model is strained in the x direction. As the simulation progresses and the model is strained further, these areas of high plastic strain join together to form bands of high plastic strain that are parallel to the solder joint/TSV interface. Voids begin to form in the bulk solder along this band and are emulated by the software in the model with the deletion of material elements. The joint begins to experience failure at just over one micron of displacement and has completely failed at a displacement of two microns. This is verified by examining the load versus displacement curve using data taken from the simulation. Note that the curve for load versus displacement terminates at just over 2 microns. This is due to the simulation being terminated before completion.

As seen in Figure 4.2, similar results are seen the 10 micron joint without underfill present. Areas of high equivalent plastic strain again begin to develop at the corners of the solder joint as the model is strained in the x direction and join together to form bands of high plastic strain that are parallel to the solder joint/TSV interface as the simulation progresses. Once again, voids begin to form in this band of high plasticity and material elements begin to be deleted as the simulation progresses and the plastic strain grows along these bands. This joint begins to experience failure at just over two microns of displacement and has completely failed at a displacement of three microns. Examining the load versus displacement curve verifies this result. Note that the load versus displacement curve terminates at just under 3.5 microns due to the termination of the simulation.

The final test case without underfill present was for a 20 micron thick solder joint. This case is unique in that the solder joint encompasses the entire space between the silicon substrates and, thus, the model does not have room for a copper landing pad at the solder joint/TSV interfaces. Because of this, the copper TSV does not have

the opportunity to participate in the deformation as much as it does in the cases with a thinner solder joint due to the fact that the joint is also sitting on the silicon substrates. This silicon substrate is far more rigid than the copper TSV. However, as seen in Figure 4.3, the results seem to indicate that this fact plays only a small role with respect to the failure evolution of the joint. As with the previous two test cases without underfill present, areas of high equivalent plastic strain begin to develop at the corners of the solder joint as the model is strained in the x direction. As the simulation progresses, these areas of high plasticity link together to form the expected bands of high plastic strain parallel to the solder joint/TSV interfaces. As before, voids begin to form in this band as strain builds up and are emulated using element deletion by the software. The joint begins to experience failure at approximately three microns of displacement and has completely failed at a displacement of 5 microns. This result is verified by examining the load versus displacement curve using data taken from the simulation. It should be noted that the simulation has been paused prior to the complete failure of the joint in order to prevent the impingement of the joint into the silicon substrate. More on this will be presented at the end of this chapter.

The test cases with underfill present provided some interesting results as can be seen in figures 4.4 through 4.6. In general, the underfill material acted as a buffer which delayed the onset of joint failure by initially concentrating the loading along the sides of the solder joint at the underfill interface. This resulted in the delamination of the underfill material, which preceded the failure of the joint. This delamination is significant with regard to failure in electronic packaging in that delamination can offer a path for electromigration and corrosion [24]. Previous work in this area has suggested that the presence of an underfill material reduces the risk of solder joint failure [2]. As was seen in Chapter 3 of this research, the presence of underfill affects the deformation pattern in the solder joint to a significant extent.

Examining the case of the 5 micron solder joint with underfill present (Figure 4.4)

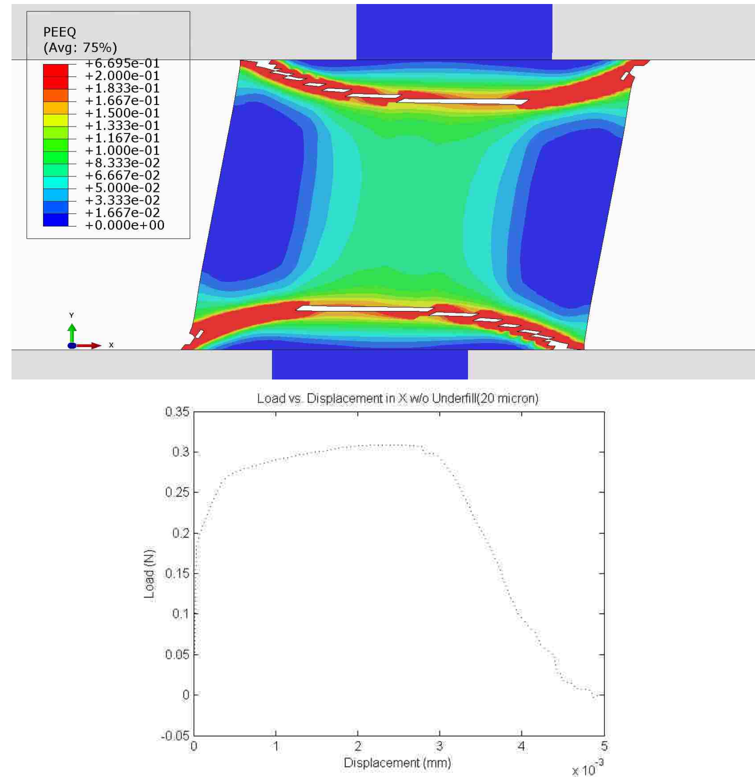

Figure 4.3: *Abaqus model showing the failure of the 20 micron solder joint without underfill present. The load versus displacement curve showing the significant drop in loading at approximately 3.5 microns indicates that the joint has failed.*

does not, at first, seem to confirm these results. As with the test cases without underfill present, a strong band of plasticity begins to develop in the bulk solder. In this test case however, voids begin to develop within the bulk solder along this band of high equivalent plastic strain and lead to the failure of the joint along this band prior to the delamination of the solder joint from the underfill material. These results are inconsistant with the first part of this research as well as the next two test cases for models with underfill present. It is believed that the coarse nature of the mesh in this particular test case is the likely culprit behind this discrepancy. More on this result will be covered at the end of this chapter.

Although the joint has failed, the load versus displacement curve appears to be nearly

linear. This is due to the fact that the underfill material continues to resist the loading after the solder joint has failed. It should be noted that the simulation has been paused prior to the complete separation of the solder joint in order to prevent the impingement of the joint into the underfill material. This seems to be a common event in all of the test cases with underfill present. More on this will be presented at the end of this chapter.

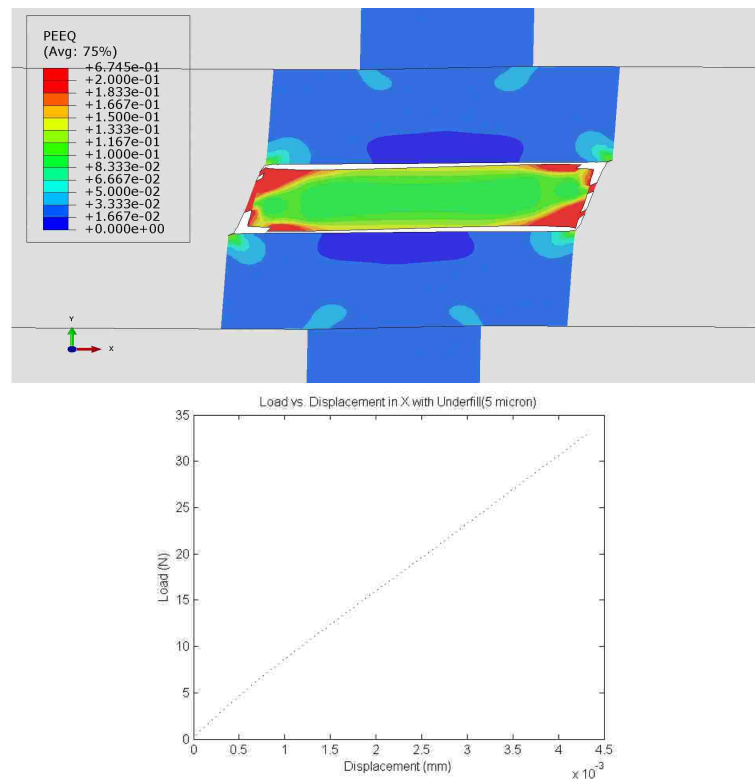

Figure 4.4: *Abaqus model showing the failure of the 5 micron solder joint with underfill present. The load versus displacement curve does not show any significant drop in loading due to the fact that the underfill material continues to resist the loading even after the joint has failed.*

As seen in Figure 4.5, the test case for the 10 micron solder joint with underfill present is very dissimilar to the 5 micron case with underfill present. As was expected from the results of the first part of this study, regions of high plastic strain develop along

the solder joint/underfill interface prior to developing in the bulk solder and lead to the eventual delamination of the solder joint and the underfill material. After delamination, the characteristic bands of high plastic strain begin to develop in the bulk solder parallel to the solder joint/TSV interfaces. As the simulation progresses, voids begin to form within these bands and eventually lead to the complete failure of the solder joint.

Unlike the previous test case with underfill present, the 10 micron solder joint does delaminate from the underfill material prior to failure, which is the expected behavior when the results of the first part of this research are considered. In addition, whereas the 5 micron case fails along both of the plasticity bands, the 10 micron joint fails only along one plasticity band. As before with the 5 micron case, the load versus displacement curve appears to be nearly linear due to the fact that the underfill material continues to resist the loading even after the joint has failed. This simulation was also paused prior to complete joint failure in order to prevent the impingement of the joint into underfill material.

The final case was for a 20 micron solder joint with underfill present. As with the 20 micron case without underfill present, the solder joint for this test case takes up the entire space between the silicon substrates and leaves no room for a copper TSV landing pad. However, the experimental results do not seem to have been affected by this fact. As seen in Figure 4.6, regions of high equivalent plastic strain first develop at the solder joint/underfill interfaces as expected and lead to the eventual delamination of the solder joint from the underfill material. After delamination has occurred, the signature bands of plasticity begin to form in the bulk solder as the simulation progresses. This simulation was the only one of the test cases for this part of the study that actually displaced the entire 5 microns in the x direction.

This particular test case displays features from the preceding case and is also consistent with the first part of this research. Much like the 10 micron case with underfill, the solder joint has delaminated completely from the underfill material prior to the

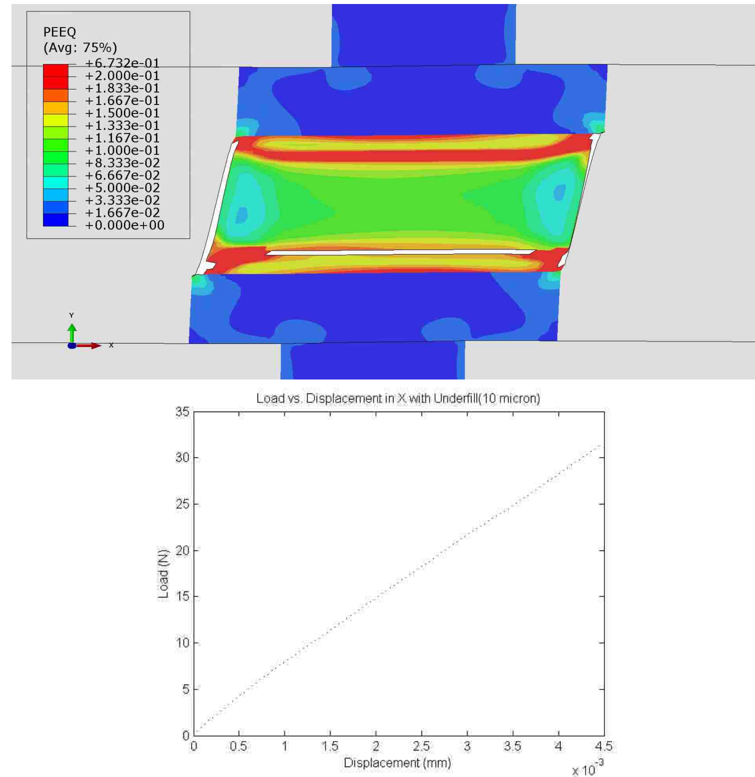

Figure 4.5: *Abaqus model showing the failure of the 10 micron solder joint with underfill present. The load versus displacement curve does not show any significant drop in loading due to the fact that the underfill material continues to resist the loading even after the joint has failed.*

formation of the bands of high equivalent plastic strain within the bulk solder, which was expected. It should be noted that this simulation completed prior to the formation of voids within the bulk solder. However, the bands of high equivalent plastic strain parallel to the solder joint/TSV interfaces are clearly visible identifying the paths of eventual failure. As with the previous two cases with underfill, the load versus displacement curve appears to be nearly linear due to the fact that the underfill material continues to resist the loading even after the joint has failed.

In order to reconcile the fact that the simulation for the 5 micron solder joint with underfill present did not give results consistant with the first part of this research,

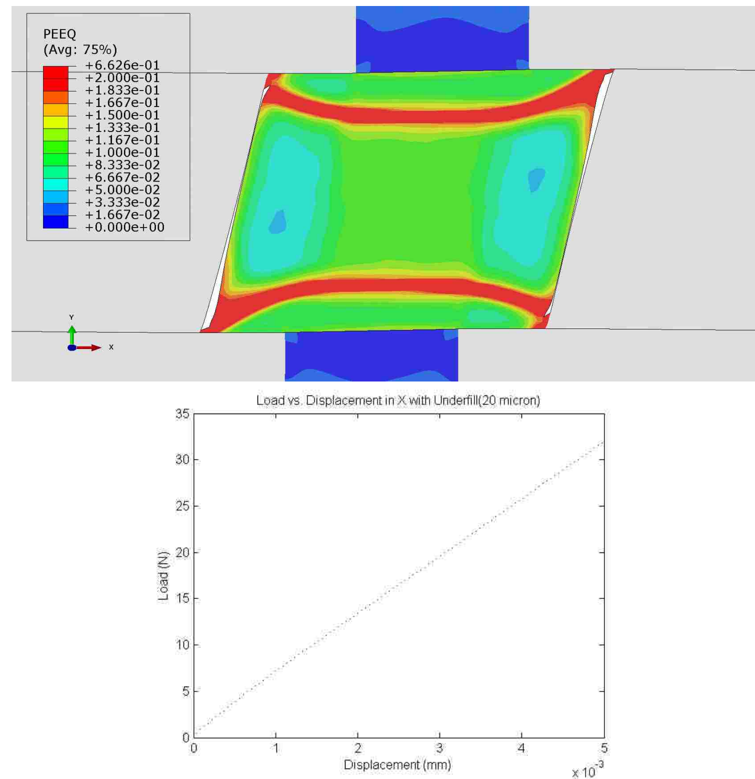

Figure 4.6: *Abaqus model showing the failure of the 20 micron solder joint with underfill present. The load versus displacement curve does not show any significant drop in loading due to the fact that the underfill material continues to resist the loading even after the joint has failed.*

an additional model was constructed with a finer mesh in order to check the validity of the results produced by the simulations. This was done in order to provide a finer mesh for the much smaller 5 micron solder joint. The new model utilized the same materials and material properties as the models with the coarser mesh. The only difference in the model was that it utilized twice as many mesh nodes in the x and y directions. This resulted in four times as many mesh elements in the solder, thus giving a much finer mesh in the area of interest. As was expected from the higher number of elements in the model, the computational time was similarly increased. Due to this fact, only a limited number of experimental runs were possible. The

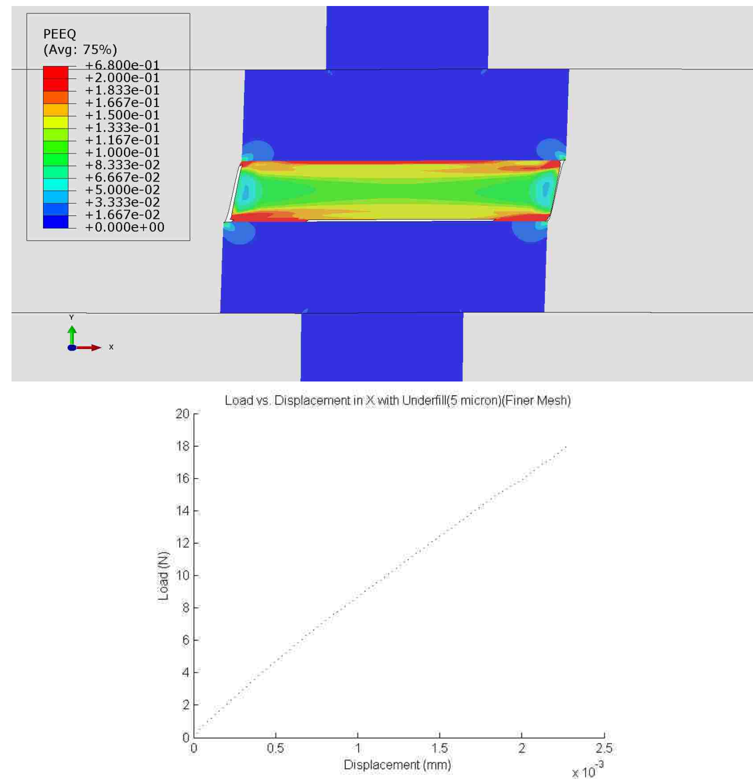

Figure 4.7: *Abaqus model of the 5 micron solder joint with underfill present. This model utilized a much finer mesh incorporating four times the number of elements used in the other test case models. The results of the simulation are much more in agreement with the other two test cases with underfill present. A plot of load versus displacement is included for comparison.*

resulting model with the finer mesh did produce results that were more consistent with the 10 and 20 micron solder joints with underfill present as well as the first part of this research. The results showed that the 5 micron joint does delaminate from the underfill material prior to the failure of the solder joint. As expected, after the delamination of the solder joint from the underfill material, bands of high equivalent plastic strain develop in the bulk solder and, as the simulation progressed, voids begin to form in the band and lead to the eventual failure of the solder joint.

In the test cases for a 10 and 20 micron solder joint, the solder is thick enough to include a sufficient number of elements in the numerical model so mesh dependency

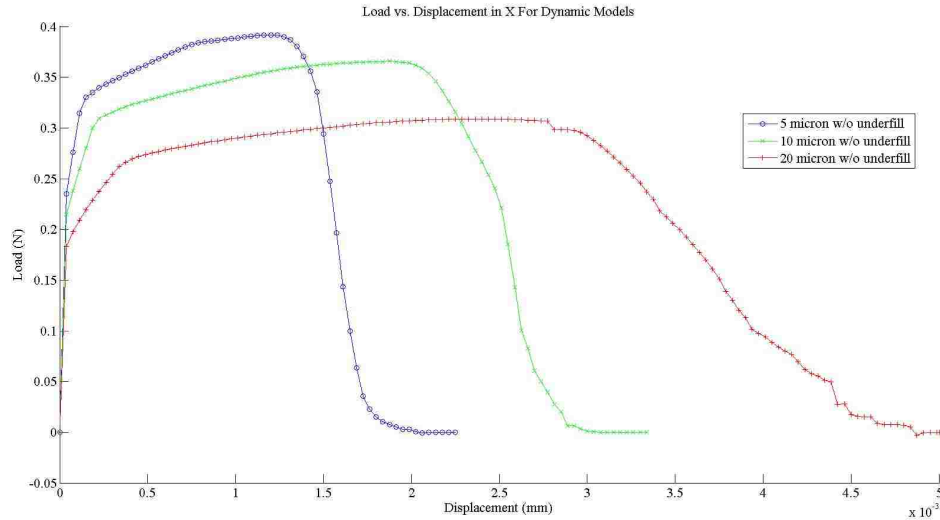

Figure 4.8: *Plots of load versus displacement for the test cases without underfill present. Note that although the 5 micron solder joint has failed first, it actually resisted a higher loading before failure.*

does not become an issue. The original numerical model for the 5 micron solder joint contained approximately 1000 elements within the solder joint mesh. The results of the simulation indicate that this is an insufficient number of elements for accurate failure modeling when underfill material is present. The numerial model for the 10 micron solder joint contained twice this number of elements in the solder mesh- approximately 2000 elements. The numerical model for the 20 micron solder joint contained four times the number of elements in the solder joint mesh than were present in the 5 micron solder joint numerical model- approximately 4000 elements. The pausing of a simulation prior to the impingement of the solder joint into the underfil material or silicon substrate was done in order to maintain the fidelity of the simulations. While this impingement can occur in physical models, the current simulation was not programmed to account for how this impingement would alter the stress and strain fields in the model. In essence, the software used to simulate these test cases simply ignored the fact that two pieces of the same model were en-

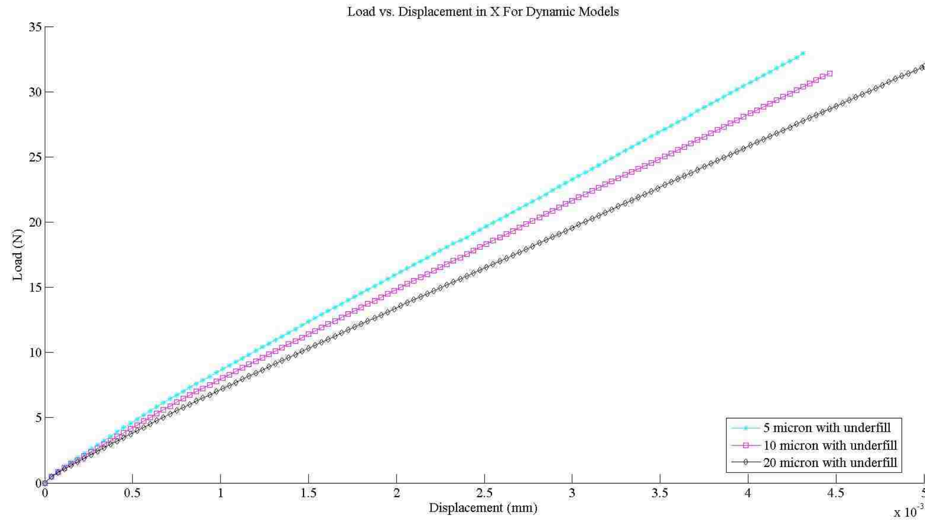

Figure 4.9: *Plots of load versus displacement for the test cases with underfill present. Note that the 5 micron solder joint is able to resist a higher loading than the 10 or 20 micron solder joints.*

countering each other and allowed the pieces to overlap with each other while not affecting the stress and strain fields of the model. This is an obvious issue considering the fact that two pieces of material that are in contact with other will impose forces on each other. These forces can and will interact with forces currently at work in the surrounding material where contact is occurring and may greatly influence the direction and magnitude of these forces. Some forces may be cancelled out entirely while other forces may be redirected into parts of the model that were previously at an equilibrium with surrounding forces. Needless to say, this contact can not be ignored as it may greatly affect the evolution of failure in the solder joint. For these reasons, it was decided that the simulations should be paused prior to the impingement of two material such as the solder joint into the much softer underfill material or the solder joint into the much harder silicon substrate. While it may be possible to program the model so that such an overlap would not be allowed to occur and two pieces of the same model would instead be assumed to be in contact with each

other, such an approach was not attempted in the present study.

The results of this part of the research indicate that having underfill material present plays an interesting role in the evolution of failure within the solder joint. According to the data provided in the simulations, the test cases with underfill present actually begin to experience failure before the corresponding test case without underfill present. Tables for this data can be found in the conclusions section of this report. This failure comes in the form of the delamination of the solder joint from the underfill material along the interfaces. After complete delamination from the underfill, the solder joint is now in essence a solder joint without underfill material present as the underfill can no longer influence the stress and strain fields of the bulk solder material. In this way, the presence of underfill material serves to delay the onset of failure in the solder joint but, as the underfill is no longer physically bonded to the joint, does nothing to actually strengthen the joint. In addition, as was pointed out earlier, this delamination can lead to electromigration and/or corrosion and, thus, can actually increase the chances of the solder joint failing.

In reference to the thickness of a solder joint, it is seen from the plots of load versus displacement for both the test cases with and without underfill present, Figures 4.8 and 4.9, that the 5 micron solder joint thickness was consistently able to withstand a higher loading than the 10 or 20 micron solder joint thicknesses. Even without underfill present, where the 5 micron joint can be seen to fail before the 10 or 20 micron solder joints, the 5 micron joint is able to resist a higher loading before experiencing failure. In terms of misalignment induced shear or a drop impact, this would seem to indicate that the thinner solder joint has a higher chance of resisting failure than would a thicker solder joint. The presence of an underfill material seems to have no impact on this observation.

Despite these salient observations, overall results indicate that the test cases with underfill material present were able to withstand larger amounts of horizontal strain than the test cases without underfill present. This is evident when examining the

plots of load versus displacement for both sets of test cases. As can be seen by examining the axis for load, which is in Newtons, the test cases with underfill present display a load scale that is a full two orders of magnitude higher than the test cases without underfill present. While it can be argued that the difference in load scales can be attributed to the fact that the underfill material continued to resist the loading even after the joint has failed, it must also be considered that this fact may actually serve to prevent failure in the neighboring solder joints by helping to dampen the transmission of bending strain through the electronic packaging as opposed to allowing it to be transmitted directly into the adjacent solder joints. It must also be considered that the test case for the 20 micron solder joint with underfill present did not experience failure in the bulk solder even after a displacement of the full 5 microns in the horizontal direction. In the end, the final judgement on the benefits versus cost of underfill material will have to be weighed along with other aspects of underfill material and their commiserate costs and benefits. More on this will be discussed in the conclusion of this paper.

Chapter 5

Concluding Discussion

The report examined two aspects of solder joint modeling for 3D IC packaging. The first aspect dealt with a periodic boundary condition that was found to be noticeably absent in nearly all research focused on modeling the behavior of solder joints when subjected to drop impact or misalignment induced shear. The second aspect of this research dealt with the evolution of failure within the solder joint when subjected to a horizontal shear condition. Both aspects of this research also examined how the presence of underfill material would affect the respective results. The conclusions of this research are presented here.

Table 5.1: Failure Time And Displacement Without Underfill Present

Solder Thickness	Failure Time	Displacement
5 micron	.034 sec	1.7 micron
10 micron	.048 sec	2.4 micron
20 micron	.056 sec	2.8 micron

With regard to the addition of a periodic boundary condition, results would indicate that it is favorable to include a periodic boundary condition when the model contains underfill material. This is readily apparent when examining the test cases of all solder joint thicknesses with underfill present. The test cases without the periodic

Table 5.2: Failure Time And Displacement With Underfill Present

Solder Thickness	Failure Time	Displacement
*5 micron	.028 sec	1.4 micron
10 micron	.044 sec	2.2 micron
20 micron	.052 sec	2.6 micron

* Results using finer mesh

boundary condition display von Mises and shear stress fields that, although symmetric about the copper TSV, are somewhat chaotic throughout the underfill material and silicon substrate. In addition, there are unusual stress concentrations at the corners of the model and, in some cases, at the underfill/substrate interfaces. The test cases with the periodic boundary condition added display much more continuous and uniform von Mises and shear stress fields and have no such stress concentrations. The test cases without underfill present do not seem to be affected by the introduction of a periodic boundary condition. None of the stress or strain fields for these test cases display significant differences between the cases that included the boundary condition and those that did not. In fact, when examining the plots of load versus displacement for these test cases, the plot for the test case with the periodic boundary condition seems to fall on top of the plot for the test case without the boundary condition. Because of this fact, it can be said that the load response of both test cases are identical when there is no underfill material present whether a periodic boundary condition is imposed or not.

It is interesting to note that the equivalent plastic strain fields for all test cases in the first part of this research, both with and without underfill present, were not significantly affected by the presence of a periodic boundary condition. While there were slight differences in peak plastic strain recorded, this increase was only approximately five percent higher with the test cases that utilized a periodic boundary condition with underfill present. The equivalent plastic strain fields for the test cases that did not have underfill present and did not utilize a periodic boundary condition were virtually indistinguishable from the test cases without underfill that did not

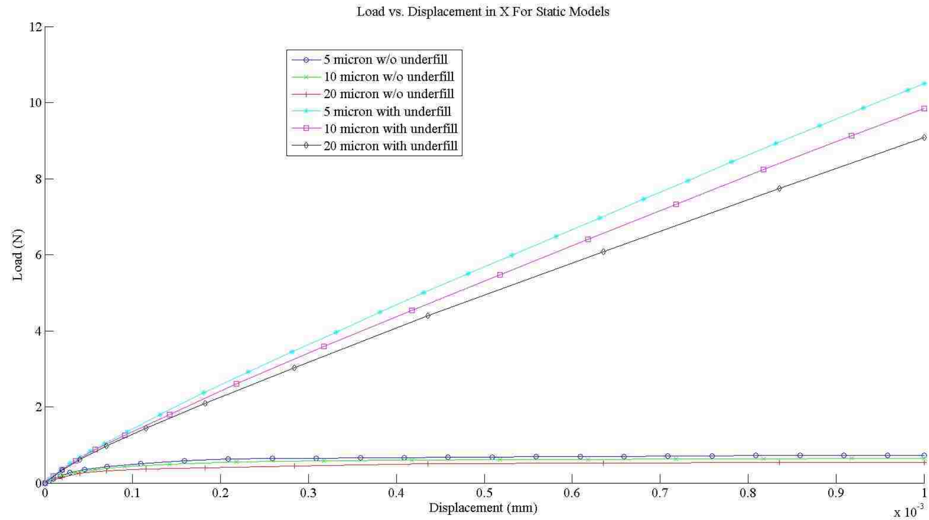

Figure 5.1: *Plots of load versus displacement for all of the test cases in the first part of this research. Note that the 5 micron solder joint with underfill present is able to resist a higher loading than any of the other test cases.*

utilize the boundary condition. Therefore, it was decided that utilizing this periodic condition was unnecessary in the second part of this research as equivalent plastic strain would be the primary indication of failure in the solder joint.

It should be mentioned that the results of this part of the research also indicate that having underfill material present in the solder joint increases its ability to resist loading. This is reinforced by the fact that the plots of load versus displacement for the test cases without underfill material present display a load scale that is a full order of magnitude smaller than the plots of the test cases with underfill present. Moreover, the curves for the test cases without underfill present show a distinct leveling off while the test cases with underfill display much more linear characteristics. This is confirmed when all of the test cases for the first part of this research are plotted together.

The second part of this study dealt with the evolution of damage in the solder joint when placed under a horizontal shear condition. These results suggest that failure

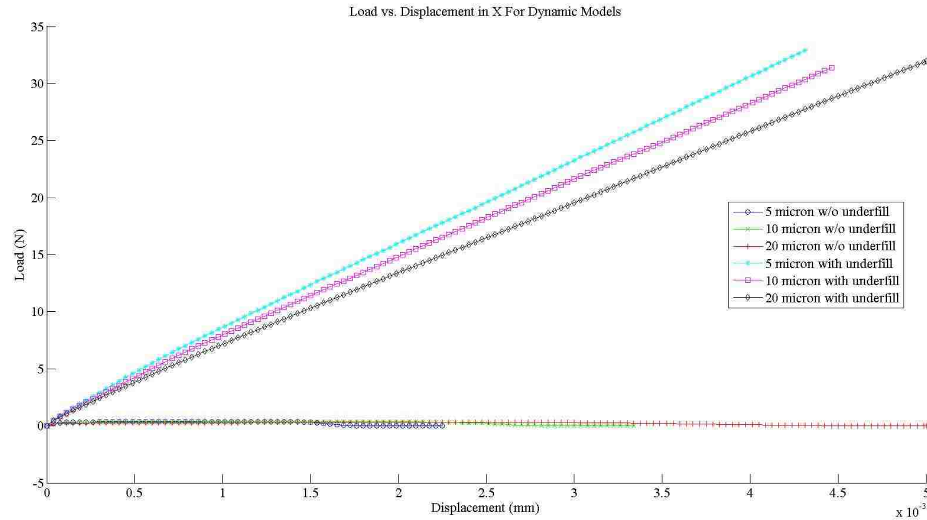

Figure 5.2: *Plots of load versus displacement for all of the test cases in the second part of this research. Note that the 5 micron solder joint with underfill present is able to resist a higher loading than any of the other test cases.*

within the bulk solder material is preceded by the formation of bands of high equivalent plastic strain. These bands initiated at the corners of the solder joint and eventually linked together as the strain in the bulk solder increased. After linking had occurred, voids began to form in the bulk solder within these plasticity bands and led to the eventual failure of the solder joint as the simulation progressed.

The presence of underfill material served to delay the formation of these bands of high equivalent strain by concentrating the plastic strain at the solder joint/underfill interfaces. This concentration led to the eventual delamination of the solder joint from the underfill material. After this delamination occurred, the solder joint was essentially the same as its respective solder joint thickness without underfill present at which time the continued horizontal straining of the model led to the formation of the characteristic plasticity bands. With continued straining, voids would form in these bands and lead to the eventual failure of the bulk solder material.

Both parts of this study support the observation that the utilization of a thinner

solder joint allows the 3D IC packaging to withstand a higher level of horizontal shear loading than would the utilization of a thicker joint. This result is supported by figures 5.1 and 5.2. These plots clearly show that the 5 micron solder joint was able to resist a higher loading than either the 10 or 20 micron joints of the respective test cases. In fact, in both figures the 5 micron joint with underfill present resists a higher loading than any of the other test cases.

It is important to mention at this point that the delamination of the underfill material from the bulk solder material and a failure within the bulk solder material, although two different events, can both be characterized as solder joint failure. As was mentioned earlier in this report, delamination of the underfill material can lead to electromigration and/or corrosion within the solder joint. Both of these can result in the failure of the solder joint. And, of course, if the bulk solder joint develops a crack that propagates through the bulk solder material, the joint can also said to have failed.

This is an important consideration when it is taken into account the fact that having the underfill material present produced a solder joint that was capable of withstanding a higher loading than its respective solder joint thickness without underfill present. As seen tables 5.1 and 5.2, the solder joints with underfill present began to delaminate before voids began to form in the respective solder joints without underfill present. As this delamination can also be characterized as failure, it can be argued that the solder joints with underfill present actually began to experience failure before the solder joints without underfill. But, it must also be pointed out that the underfill material continued to resist the shear loading even after the bulk solder material had failed. This is an important fact when considering that these solder joints are part of a larger part, the 3D IC packaging. Underfill material can help to reduce the chances of joint failure in adjacent solder joints by damping the forces produced by misalignment induced shear or drop impact even after its respective joint has failed. This can be especially beneficial in 3D IC packaging if certain

sacrificial joint with underfill material were placed on the perimeter of more critical solder joints. In this way, these joints can bear the brunt of shear forces and still continue to dampen any these forces after they have failed. In addition, when issues such as the removal of heat from the 3D IC packaging are considered, utilizing underfill material capable of conducting heat efficiently and quickly becomes even more beneficial.

In conclusion, the results of this study seem to indicate that the benefits of using underfill in 3D IC packaging outweigh the costs of doing so. They also indicate that if FEA modeling is to be used to examine the behavior of this packaging under misalignment induced shear or drop impact, it is beneficial to include a periodic boundary condition in order to improve the fidelity of the analytical results. In addition, results would seem to indicate that using a thinner solder joint can allow the 3D IC packaging to withstand a higher horizontal shearing force before failing than would using a thicker solder joint.

References

[1] K.N. Tu, "Reliability challenges in 3D IC packaging technology," *Microelectronics Reliability*, 51(3) pp. 517-523 March 2011

[2] Y.-L. Shen and R.W. Johnson, "Misalignment induced shear deformation in 3D chip stacking: A parametric numerical assessment," *Micrelectronics Reliability*, 53(1) pp. 79-89 January 2013

[3] S.H. Lee, K.-N. Chen, and J. Lu, "Wafer-to-Wafer Alignment for Three-Dimensional Integration: A Review," *Journal of Microelectricalmechanical Systems*, 20(4) pp. 885-898, August 2011

[4] T.S. Cale, J.-Q. Lu, and R.J. Gutmann, "Three-Dimensional Integration in Microelectronics: Motivation, Processing, and Thermomechanical Modeling," *Chemical Engineering Communications*, 195(8) pp. 847-888 August 2008

[5] C.-T. Kuo, M.-C. Yip, and K.-N. Chiang, "Time and temperature-dependent mechanical behavior of underfill materials in electronic packaging application," *Microelectronics Reliability*, 44(4) pp. 627-638, April 2004

[6] Y.-L. Shen, "Externally constrained plastic flow in miniturized metallic structures: A continuum-based approach to thin films, lines, and joints," *Progress in Materials Science*, 53(5) pp. 838-891 July 2008

[7] W.J. Plumbridge, "Solders in electronics," *Journal of Materials Science* 31(10) pp. 2501-2514 May 1996

[8] Directive 2002/95/EC of the European Parliament and of the Council of 27 January on the restriction of the use of certain hazardous substances in electrical and electronic equipment. [Online]. Available: http://eur-lex.europa.eu/LexUriServ/LexUriServ.do?uri=OJ:L:2003:037:0019:0023:en:PDF

[9] W.J. Tomlinson and A. Fullylove, "Strength of tin-based soldered joints," *Journal of Materials Science*, 27(21) pp. 5777-5782 November 1992

[10] E.H. Wong, C.S. Selvanayagam, S.K.W. Seah, W.D. van Driel, J.F.J.M. Caers, X.J. Zhao, N. Owens, L.C. Tan, D.R. Frear, M. Leoni, Y.-S. Lai, and C.-L. Yeh, "Stress-strain characteristics of tin-based solder alloys at medium strain rate," *Materials Letters*, 62(17-18) pp. 3031-3034, June 2008

[11] E.H. Wong, C.S. Selvanayagam, S.K.W. Seah, W.D. van Driel, J.F.J.M. Caers, X.J. Zhao, N. Owens, L.C. Tan, D.R. Frear, M. Leoni, Y.-S. Lai, and C.-L. Yeh, "Stress-Strain Characteristics of Tin-Based Solder Alloys for Drop-Impact Modeling," *Journal of Electronic Materials*, 37(6) pp. 829-836 June 2008

[12] C.S. Selvanayagam, J.H. Lau, X. Zhang, S.K.W. Seah, K. Vaidyanathan, and T.C. Chai, "Nonlinear Thermal Stress/Strain Analyses of Copper Filled TSV(Through Silicon Via) and Their Flip-Chip Microbumps," *IEEE Transactions on Advanced Packaging*, 32(4) pp. 720-728 November 2009

[13] Y.-L. Shen, N. Chawla, E.S. Ege, and X. Deng, "Deformation analysis of lap-shear testing of solder joints," *Acta Materialia*, 53(9) pp. 2633-2642, May 2005

[14] T.T. Mattila and J.K. Kivilahti, "Reliability of Lead-Free Interconnects under Consecutive Thermal and Mechanical Loadings," *Journal of Electronic Materials*, 35(2) pp. 250-256 February 2006

[15] K.N. Tu, F. Ku, and T.Y. Lee, "Morphological stability of solder reaction products in flip chip technology," *Journal of Electronic Materials*, 30(9), pp. 1129-1132 September 2001

[16] W.H. Moy and Y.-L. Shen, "On the failure path in shear-tested solder joints," *Microelectronics Reliability*, 47(8) pp. 1300-1305 August 2007

[17] M. Modi, C. McCormick, and N. Armendariz, "New Insights in Critical Solder Joint Location," *2005 Electronics Components and Technology Conference*, pp. 977-982 May 31-June 3 Lake Buena Vista, Florida, USA

[18] J.-W. Jang, A.P. De Silva, J.E. Drye, S.L. Post, N.L. Owens, J.-K. Lin, and D.R. Frear, "Failure Morphology After Drop Impact Test of Ball Grid Array (BGA) Package With Lead-Free Sn-3.8Ag-0.7Cu and Eutectic SnPb Solders," *IEEE Transactions on Electronics Packaging Manufacturing*, 30(1) pp. 49-53 January 2007

[19] Y. Yao and L.M. Keer, "Cohesive fracture mechanics based numerical analysis to BGA packaging and lead free solders under drop impact," (2013), *http://dx.doi.org/10.1016/j.microrel.2012.12.007*

[20] Y.-L. Shen and K. Aluru, "Numerical study of ductile failure morphology in solder joints under fast loading conditions," *Microelectronics Reliability*, 50(12) pp. 2059-2070 December 2010

[21] F. Ochoa, J.J. Williams, and N. Chawla, "Effects of cooling rate on the microstructure and tensile behavior of a Sn-3.5 wt%Ag solder," *Journal of Electronic Materials*, 32(12) pp. 1414-1420 December 2003

[22] P. Lall, S. Gupte, P. Choudhary, and J. Suhling, "Solder Joint Reliability in Electronics Under Shock and Vibration Using Explicit Finite-Element Submod-

eling," *IEEE Transactions on Electronics Packaging Manufacturing*, 30(1) pp. 74-83 January 2007

[23] C.-K. Lee, T.-C. Chang, Y.-J. Huang, H.-C. Fu, J.-H. Huang, Z.-C. Hsiao, J.H. Lau, C.-T. Ko, R.-S. Cheng, P.-C. Chang, K.-S. Kao, Y.-L. Lu, R. Lo, and M.J. Kao, "Characterizations and Reliability Assessment of Solder Microbumps and Assembly for 3D IC Integration," *2011 IEEE Electronic Components and Technology Conference*, pp. 1468-1474 May 31-June 3 Hsinchu, Taiwan

[24] Q. Tong, B. Ma, A. Xiao, and A. Savoca, "Fundamental adhesion issues for advanced flip chip packaging," *2002 IEEE Electronic Components and Technology Conference*, pp.1373-1379 May 31 San Diego, CA USA

[25] C. Kung, T.-T. Liao, and C.-H. Liao, "Parametric Analyses on Fatigue Reliability of 3D IC Packages with Built Through Silicon Vias (TSVs)," *2012 International Conference on Mechatronics and Automation*, pp. 121-126 August 5-8, Chengdu, China

[26] A. Guedon-Garcia, E. Woirgard, and C. Zardini, "Reliability of Lead-Free BGA Assembly: Correlation Between Accelerated Ageing Tests and FE Simulations," *IEEE Transactions on Device and Materials Reliability*, 8(3) pp. 449-454 September 2008

[27] J.K. Kivilahti and K. Kulojärvi, "Design and Reliability of Solders and Solder Interconnections," ed. R.K. Mahidhara, (Warrendale, PA: TMS, 1997), pp. 377-384

[28] J. H. Lau, "Overview and outlook of through-silicon via (TSV) and 3D integrations", *Microelectronics International*, 28(2), pp. 8-22 2011

[29] ABAQUS 6.8, Users Manual, Dassault Systémes Simulia Corp., Providence, RI

[30] J. Guthrie, M.S. Project Report, University of New Mexico; 2012

[31] Y.-L. Shen, "Constrained deformation of materials," New York: Springer; 2010

[32] L. J. Ladani, "Numerical analysis of thermo-mechanical reliability of through silicon vias (TSVs) and solder interconnects in 3-dimensional integrated circuits," *Microelectronic Engineering*, 87(2) pp. 208-215 February 2010

[33] S.-H. Hwang, B.-J. Kim, H.-Y. Lee, and Y.-C. Joo, "Electrical and Mechanical Properties of Through-Silicon Vias and Bonding Layers in Stacked Wafers for 3D Integrated Circuits," *Journal of Electronic Materials*, 41(2) pp. 232-240 February 2012